AD-A079 540 HUGHES AIRCRAFT CO CULVER CITY CALIF F/G 17/8
POSITION AND ATTITUDE MONITOR (PAM).(U)
AUG 79 L HILL, W BUCHMAN, J WAGNER, R JULIAN DAAB07-75-C-0810
UNCLASSIFIED HAC-FR-79-73-801R DELNV-TR-75-0810-F NL

1 OF 2
AD A079540

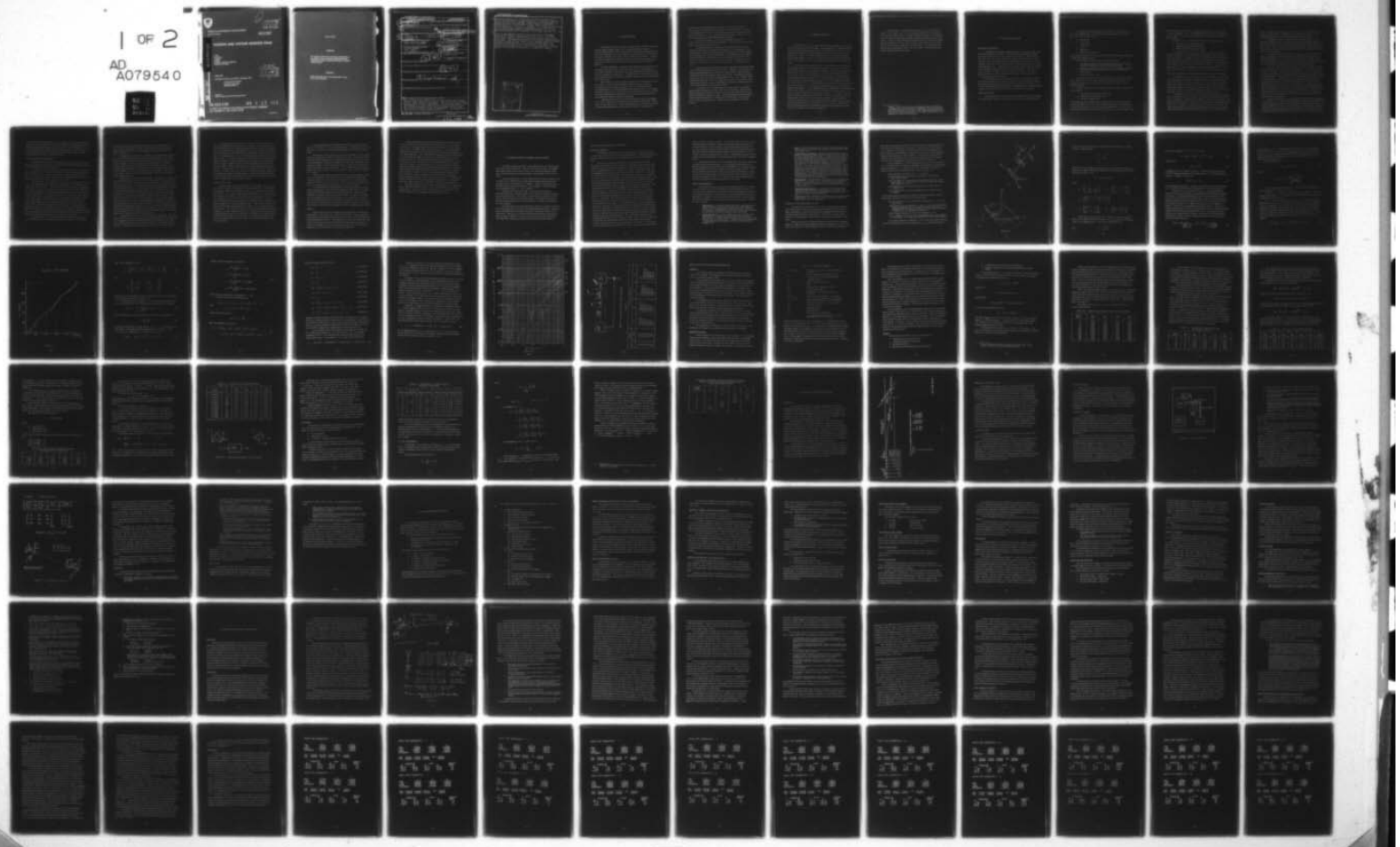

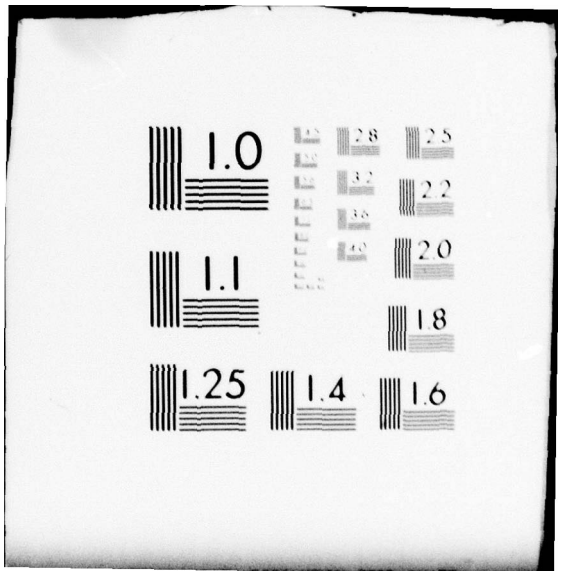
1.0
1.1
1.25
1.4
1.6
2.8
3.2
3.6
4.0
2.5
2.2
2.0
1.8

LEVEL

Research and Development Technical Report

DELNV-TR-75-0810-F

Report No. 79-73-901R
HAC Ref. No. D2493

POSITION AND ATTITUDE MONITOR (PAM)

L. Hill
W. Buchman
J. Wagner
R. Julian
HUGHES AIRCRAFT COMPANY
Culevr City, CA 90230

August 1979

Final Report for Period June 1975 to September, 1978

DISTRIBUTION STATEMENT

Approved for public release;
distribution unlimited.

Prepared for:
NIGHT VISION & ELECTRO-OPTICS LABORATORY

ERADCOM

US ARMY ELECTRONICS RESEARCH & DEVELOPMENT COMMAND
FORT MONMOUTH, NEW JERSEY 07703

NOTICES

Disclaimers

The citation of trade names and names of manufacturers in this report is not to be construed as official Government indorsement or approval of commercial products or services referenced herein.

Disposition

Destroy this report when it is no longer needed. Do not return it to the originator.

Unclassified
SECURITY CLASSIFICATION OF THIS PAGE (When Data Entered)

REPORT DOCUMENTATION PAGE	READ INSTRUCTIONS BEFORE COMPLETING FORM
1. REPORT NUMBER: DELNV-TR-75-0810-F	2. GOVT ACCESSION NO. / 3. RECIPIENT'S CATALOG NUMBER
4. TITLE (and Subtitle): Position and Attitude Monitor (PAM),	5. TYPE OF REPORT & PERIOD COVERED: Final Tech Rpt
	6. PERFORMING ORG. REPORT NUMBER: HAC-FR-79-73-801R, HAC-REF-D2493
7. AUTHOR(s): L. Hill, W. Buchman, J. Wagner, R. Julian	8. CONTRACT OR GRANT NUMBER(s): DAAB07-75-C-0810
9. PERFORMING ORGANIZATION NAME AND ADDRESS: Hughes Aircraft Company, Culver City, California	10. PROGRAM ELEMENT, PROJECT, TASK AREA & WORK UNIT NUMBERS: 1L1 62703 DH93 W2 062
11. CONTROLLING OFFICE NAME AND ADDRESS: US Army ERADCOM, ATTN: DELNV-L, Fort Monmouth, New Jersey 07703	12. REPORT DATE: August 1979 / 13. NUMBER OF PAGES: 102
14. MONITORING AGENCY NAME & ADDRESS (if different from Controlling Office)	15. SECURITY CLASS. (of this report): Unclassified / 15a. DECLASSIFICATION/DOWNGRADING SCHEDULE

16. DISTRIBUTION STATEMENT (of this Report)

Distribution Unlimited; Approved for Public Release.

17. DISTRIBUTION STATEMENT (of the abstract entered in Block 20, if different from Report)

18. SUPPLEMENTARY NOTES: Final technical rept.

19. KEY WORDS (Continue on reverse side if necessary and identify by block number)

20. ABSTRACT (Continue on reverse side if necessary and identify by block number)

The exploratory development model of the Position and Attitude Monitor, PAM, represents the current state of the art in electro-optical remote attitude measurement. The basic operation of the PAM depends on a laser illuminating retroreflective optics of the airborne component from a tracking ground station. The application for which the PAM was developed is an Airborne Passive Artillery Locating System (PALS-A).

DD FORM 1 JAN 73 1473 EDITION OF 1 NOV 65 IS OBSOLETE

UNCLASSIFIED
SECURITY CLASSIFICATION OF THIS PAGE (When Data Entered)

172300

PAM design details, test techniques, and pre-acceptance test results are presented. Formal acceptance testing was completed after delivery to Ft. Monmouth. These tests are documented in a technical report "Position and Attitude Monitor Exploratory Development" by F. Elmer and C. Joannou. Test techniques developed for the PAM by Mr. F. Elmer are presented in a paper entitled "Electrical-Optical Remote Attitude Measurement" given at the 8th Classified DOD Laser Conference in San Diego, November 15, 1978

Position measurement accuracy of the exploratory development model of the PAM was demonstrated to be 0.1 meter. Attitude measurement capability was demonstrated to on the order of 0.2 milliradian. The operational range of the PAM was demonstrated to 450 meters. All testing was done on the ground using a horizontal simulated flight profile. Test results validate PAM design concepts and indicate further development is warranted. This electro-optical, three-axis, remote attitude measuring technique appears to be useful to distances of a kilometer or more.

1.0 INTRODUCTION

The airborne Passive Artillery Location System, PALS-A is designed to locate active hostile artillery via an appropriate sensor flown on a remotely piloted vehicle, RPV, loitering several kilometers behind the lines. The sensor appropriate for this mission can accurately give the direction to the target, but only with respect to its own arbitrary orientation. A device or system is required to express the direction to the detected target in the ground coordinate system in order to locate the target for counterfire purposes.

For this application, the position and attitude measuring device must be able to locate the airborne sensor to within 1 meter horizontally and 0.5 meters vertically. This device must also determine the attitude of this sensor to within 0.25 milliradian. The flight profile of the RPV is assumed to lie within a cylinder 50 meters in diameter and between 300 and 600 meters above the terrain.

State of the art inertial systems to perform this function were ruled out as they 1. did not have the required attitude accuracy (best was 0.5 degree), 2. were costly and heavy, and 3. were subject to drift (0.1 degree/hour). The limited flight profile suggests the use of a tactical, portable ground station in conjunction with a cooperative device on the RPV. Accuracy considerations suggest the use of electro-optical techniques to accomplish the attitude measurement function.

With the above in mind, a contract was let in June 1975 to Hughes Aircraft Co. (HAC), for the exploratory development of the PAM. During the course of the contract, it became apparent that the standard techniques of measuring attitude could not be used as a basis for evaluating the

performance of the PAM. Novel techniques for testing the PAM were developed by the ERADCOM Project Engineer for the PAM, Mr. F. Elmer. These techniques were implemented during successful pre-acceptance testing at HAC in Feb. 78. As a result, this final report is written as a cooperative effort between ERADCOM and HAC personnel.

The final acceptance testing was successfully completed in September 78 at Ft. Monmouth by ERADCOM. This testing will be reported under a separate technical report.

As expected during any exploratory development program, many problems arose due to incomplete understanding of basic principles, and application of "engineering approximations" in regions where their underlying assumptions are not necessarily valid. The identification and solution of these problems constitutes the major contribution of this effort to the advancement of the state of the art and makes further development of this exploratory model into a versatile tactical subsystem a highly desirable goal.

Position measurement accuracy of the exploratory development model of the PAM was demonstrated to be 0.1 meter. Attitude measurement capability was demonstrated to the order of 0.2 milliradian. The operational range of the PAM was demonstrated to 450 meters. All testing was done on the ground using a horizontal simulated flight profile. Test results validate PAM design concepts and indicate further development is warranted. This electro-optical, three-axis, remote attitude measuring technique appears to be useful to distances of a kilometer or more.

In summary, all of the concepts for remote attitude and position measurement were shown to work, and to work in the field. If there is further development, these same concepts can be carried forward into a much smaller and totally automatic system. The PAM program has demonstrated remote attitude (and position) measurement in three axes to the accuracy that a surveyor's transit gives. In this sense, the program was a total success.

2.0 DESIGN APPROACH

The ground station, GS, sights the airborne component, AC, mounted on the RPV by means of a rifle scope. Upon acquisition, a television camera and closed loop tracking system, lock on to the platform and track it. The ground station gimbal encoders provide two of the six measured algorithm parameters. These are azimuth and elevation. The third ground station measured parameter is range. A commercial range measuring tellurometer uses a retroreflecting corner cube on the airborne platform to measure the range.

Three more measured parameters are needed to provide sufficient information to compute the attitude of the airborne component. These are the roll, pitch and yaw of the airborne component. On the entrance aperture of the corner cube is a sheet polarizer. A laser beam illuminates this corner cube. The retroreflected beam is measured by a modified commercial polarization measuring device. The return polarization is determined by the airborne component polarizing sheet. As "roll" changes, the reference polarization rotates. The polarimeter tracks these changes and provides the roll angle readout. The laser beam also illuminates two orthogonally spinning roof prisms. These prisms each have a single plane of retroreflection normal to the prism roof line. This retroreflection property allows each axis to provide independent returns of pitch and yaw. The "pitch" and "yaw" prisms return an orthogonal scan pattern. A receiver at the ground station detects these returns as they scan past its aperture. Angular position encoders sense the angles of these prisms and transmit this data over a data line to the ground station. The "pitch" and "yaw" receiver, (P&Y RCVR) gates this data stream thus providing the pitch and yaw angles with respect to the line of sight to the airborne component.

Summarizing, the PAM system measures the azimuth, elevation, range, "roll", "pitch", and "yaw" of an airborne platform with respect to a ground coordinate system. Azimuth and elevation angles are provided by encoders on the ground station gimbals. Range is sensed by a tellurometer device. "Roll" is measured using a airborne reference return polarization and the polarimeter. Pitch and yaw angles are provided by angle encoder data, a sync reference angle, and a receiver pulse. This pulse gates the encoder data at the proper "pitch" and "yaw" angles corresponding to the prisms aligned to the line of sight. *

*"Pitch", "yaw", and "roll" are used figuratively to describe the orientation angles of the airborne component. The reader should note that these terms do not carry their standardly accepted definitions in the context of this report. The reader should refer to the glossary for their exact definitions.

3.0 SYSTEM DESCRIPTION

AIRBORNE COMPONENT

The airborne component shown in Figure 2 centers on a cube corner which has a polarizer on its face. Mounted as close as possible are the spinning porro prism shafts and spinning prism mounts. These prisms are driven by an AC synchronous motor which is geared down to turn at 10 Hz (600 rpm) rate. The motor drives both shafts through a direct drive rubber coupling. The driver shaft drives the other orthogonal shaft through a bevel antibacklash gear set. Located on the end of each prism shaft, also directly driven through a rubber coupling, are the angle encoders. The data electronics and the 5 V supply are housed within the gray box. The entire optics table is covered by a white sheet metal cover. An aperture is cut over the prisms and corner cube.

Up to 600 meters of three twisted wire pairs transmit the encoder data and remote flash to the ground station. For testing purposes a fixture for mounting a theodolite above the airborne component is provided. The PAM can be remotely flashed by either a manual switch, or an optical switch mounted so as to sense when the AC passes through a given position.

GROUND STATION

The ground station is comprised of two electronics racks in portable carrying cases; a rolling 5 foot electronic rack; and the Gimbal Assembly.

The Gimbal Assembly contains all the measuring components on a two axis gimbaled table. Azimuth and elevational stepping motors drive these axes. On the table are the

1. Rifle Scope
2. TV Camera
3. Tellurometer
4. Laser
5. Polarimeter
6. Pitch and Yaw Receiver

The Gimbal Assembly is electronically connected to the computer console by a multicable umbilical bundle.

The computer console contains the following items:

1. TV display, Azimuth and Elevational Remote Manual Tracking Command Pushbuttons, and Autotracking Controls.
2. Master Power Switch Panel and Laser Power Supply. The System Simulated Flash Control is also located on this panel.
3. HP Computer.
4. Floppy Disc Drive Unit.

For normal operation the two modular electronics racks are stacked upon each other. The one which contains the polarimeter is on top. The top rack is identified as the Polarimeter console. The lower, as the Gimbal Console.

The Polarimeter console contains the following items, located from top to bottom.

1. Polarimeter Electronics and Display
2. Pitch and Yaw Electronics Box
3. DC Power Supply Panel

For testing purposes a pitch and yaw display card, can be accessed by pulling partially out the Pitch and Yaw Electronics Box. A IC on the pitch or yaw circuit board is monitored using the provided clip. The IC, to be monitored is located in the lower left hand corner of each board (lower side

is where wires are connected). The DC panel houses +20, +5, +24, -24, -12 volt dc supplies. These are monitored by selection of the appropriate switch position. The meter is monitored only for approximate voltages on a go/no go basis.

The lower rack or Gimbal console contains the following items:

1. Azimuth Tracker Electronics Box
2. Elevation Tracker Electronics Box
3. 400 Hz 120 VAC Polarimeter Supply

The pedestal cables all go to the computer rack and are then distributed to the other two racks and within the computer rack. Power, as well, is inputted to the computer rack and distributed to the two electronics racks and teletype. All cables and connectors are identified by number, letter, and set of numbers, as well as word identification. The first number corresponds to the panel number 1 pedestal, 2 computer, 3 polarimeter pitch and yaw, 4 tracker electronics. Letter to panel connector J or cable connector P. The set of numbers corresponds to the various functions.

AZIMUTH, ELEVATION, GIMBALLED PEDESTAL, AND TV TRACKING

The ground station measuring devices are mounted on an optics table. This optics table is gimbaled on a modified Carson astronomical tracking mount, which gives the table two degrees of freedom. Modifications were made to the stepper motor drive and angular encoder package to attain for the pointing accuracy required and to integrate with the TV closed loop tracking electronics. This gimbaled motion provides two of the six measured quantities. These are azimuth and elevation of the line of sight.

The stepper motors are driven by two separate electronics packages. One for azimuth and one for elevation. These are located in the gimbal console. On/off power, stepper motor oscillator, stepper motor direction, and speed or stepper motor on, switches are provided on the front panels of these drive boxes. In addition variable speed (slow for tracking, and faster for rapid position changes) is adjusted by a potentiometer on each front panel. Additional left/right, up/down command switches are provided on the front

panel, TV display in the computer console and a remote box attached to the ground station pedestal. In addition, error signals generated by the TV tracking electronics control the drive during automatic tracking.

The encoders provide 16 bit gray code information directly to the computer interface cards. This data is processed by the PAM computer program to provide the elevation and azimuth of the ground station reference line of sight. The elevational drive contains in addition a clutch mechanism. Care should be taken to avoid unintentional rotation of this gimbal since reference zeros are destroyed.

The ground station pedestal must be aligned to provide known ground station co-ordinates. Gravity reference vertical is the primary axis to which the gimbaled axes are aligned. A precision table is attached to the elevational rotation axis using a precision level, the ground station is aligned to gravity vertical by adjustment of the ground station tripod feet.

The optics table must be pointed to the ground and leveled. By placing the level on the back surface of the optics table, in two gimbal axis, and slewing the gimbal, leveling will be accomplished. Now by using the first surface retroreflection off an opaque liquid, the pointing of the laser relative to the optics table is adjusted and set. The following alignment must be done in a darkened area. Slew the gimbal in elevation until the optics table is approximately 90 degrees from the previous position. Set the level at 90 degrees on the back surface again and adjust. At an appropriate distance away mark the position of the laser. Place the polarimeter illuminator in place, turn off laser, and view the projected light relative to the laser mark. Adjust the polarimeter package relative to the laser mark. Readjust the laser to the mark and alignment of the polarimeter package relative to the gimbal axis is accomplished.

Since the TV interface with the gimbal operation it will be discussed in this section. A TV camera with zoom lens, is mounted on the optics table. It is boresighted to the laser beam, PCY RCVR, and polarimeter axes. The electronic both for TV control, and tracking are contained in the white box attached to the base of the ground station pedestal. The TV image is displayed on the monitor located in the computer console. On this same panel

are located the tracking controls. The track/scan switch initiates automatic tracking in the track position. In the scan position, it enables control of the pedestal azimuth and elevation using the various command pushbuttons. The second switch from the right is the white/black control. The TV tracker is a contrast tracker and will track these targets with white target on black background and vice versa, using this switch.

POLARIZATION MEASUREMENT

The polarimeter detects the polarization of the returning energy from the laser illuminated corner cube. Its closed loop system detects this polarization and tracks the changing roll angle.

The output laser is retroreturned from the corner cube. The output laser is polarized and for best performance the airborne component reference axis, of the corner cube polarizing material, should be aligned parallel to this laser output polarization. The polarimeter photomultiplier tube senses the return polarization and the analyzer servo tracks it.

The electronics of the polarimeter consist of two amplification stages, a two stage digital filter and error signal amplification. The input energy is detected by a PMT detector. The first stage is transimpedance, multiplying the detector current to a suitable processing voltage level. The second stage is a low pass amplifier. The signal then divides to two parts. An integrating rectifier determines the received energy level and controls the PMT voltage level. The Faraday coil imports a time varying polarization which functions as the error signal. The digital filters, separate the first (400 Hz) and second (810 Hz) harmonics. A null is indicated by zero first harmonic. Zero is thus achieved by adjustment of the polarimeter analyzing prism to 90 degrees to the reference polarization axis. At this point a minimum in 800 Hz error signal is achieved. The closed loop response of the polarimeter drives consistantly towards the minimum first harmonic and maximum second harmonic, to align itself with the return reference polarization.

The digital filters are sequentially indexed so that monitoring represents a stepped response indication of the received waveform. The output

of the first harmonic digital filter is monitored to show acquisition of the null. This is indicated by the 400 Hz error signal gradually becoming distorted (400 Hz +800 Hz), and eventually becoming a relatively pure 800 Hz waveform.

The polarimeter operation is as follows. The polarimeter reference test fixture puts the output laser beam into the polarimeter. A rotatable preset reference polarizing sheet, provides the polarimeter with a strong polarized output. The servo acquires this polarization by rotating the analyzer until a minimum DC signal level is detected by the PMT. The oscillating magnetic field of the Faraday cell causes the input polarization vector to dither about the reference position. The result is a detected AC error signal. Once the servo has achieved null, rotate loss of signal pot until red light comes on.

Adjustment must be made mechanically. By looking in the back of the polarimeter you will see a gear train, and by alignment of the appropriate marks, the final zero set has been made. Depress the reset button zeroing the polarimeter display. The servo motor has a control winding which has two series switches in it. A manual switch is used to disable the servo loop. It is located in the polarimeter electronics and accessible from the back access panel. A second relay switch senses the return signal energy and disables the servo loop when insufficient signal is being received. These controls are necessary, since without signal the servo loop will continue to drive off null in a scan mode. Field scintillation and taking on and off the reference fixture cause large signal variations. A front control potentiometer controls the signal level at which the servo is deactivated. Weaker signals clockwise, stronger anticlockwise. It is advisable to turn the pot anticlockwise to disable loop when putting the reference fixture in place, or when the polarimeter measurements are not being made.

The polarimeter is now zeroed, and ready for operation. The reset button should not be depressed again, or the polarimeter turned off following this alignment procedure until measurements are completed. The polarimeter display is the output of a counting encoder, not an absolute position encoder. It simply measures changes in angle from a reference position.

Several points must be stressed about the polarimeter operation. We have mentioned the alignment and zero setting. Care must be taken to assure that the PMT tube is properly aligned and sensing maximum signal. This is accomplished by monitoring the received error signal, by rotation and vertical motion of the tube within its housing and seeking the maximum signal. The polarimeter is a very sensitive instrument and measures small signal levels. Too strong a signal can sometimes lock the automatic PMT voltage control in a minimum position and no signal is observed. Should this lockup occur, block the input beam into the polarimeter and hold for several seconds. Slowly unblock this beam and the signal should again be observed. The polarimeter has the narrowist FOV of the measuring components. It is thus used as the reference to which all the other components are aligned. By using a light bulb fixture, at night, the polarimeter FOV can be visually observed by looking back into the ground station. The other devices are then made to have colinear FOVs.

"PITCH" AND "YAW"

The two angles relative to the lines of sight, "pitch" and "yaw" are measured by a prism retro return, and angle encoder data. Two spinning roof prisms, rotate about orthogonal x and y axes. The spin rate is ten hertz (10 Hz). The angular prism angles about these axes are monitored by the pitch and yaw encoders. This position, with respect to a sync or reference position, is transmitted to the pitch and yaw electronics. These electronics decode the angular position as a function of time, providing a continuous monitor of the angle in digital counters. When the prism retro axis aligns with the illuminating laser line of sight, a return is detected by the P&Y receiver. The signal is detected by the Meret photodiode-transimpedance amplifier, is further amplified and drives a variable reference comparator. A digital latching signal is thus generated, transmitted to the angle counters, and latches the present count. The angle, with respect to the pitch reference is thus locked into the counter which corresponds to alignment of the retro return axis.

The roof prisms have two dimensional returns, but only a single plane of retro return. Thus each prism provides a sweeping return for only one axis. The retro return plane is perpendicular to the roof line of the prism.

The encoder output consists of two separate signals. The sync pulse (reference angle) and a 90 kHz (at 10 Hz) data stream. The two signals are combined to be transmitted over a single twisted pair line per axis. This is accomplished by using the sync-pulse to generate a missing pulse in the angle data stream. The processing electronics, then decode this process, regenerating the sync and encoder data. The encoded data is impressed on the data line (up to 600 meters) by a line driver, and received by a digital line receiver.

The only adjustment at the ground station is the threshold of the P&Y receiver comparator. It should be set as low as possible, but still discriminate against the noise on the received signal. It is a field of adjustment located on back of P&Y receivers. Care must be taken that the prism scans are orthogonal during alignment of the airborne component.

The received P&Y latching signals can be monitored using a differential scope plug-in by monitoring the appropriate BNC outputs. The data coming from the P&Y encoders can also be monitored. The pulses are extremely fast (pulse width decreases with range). Usually on a 20 millisecond scale both the pitch and yaw returns can be monitored. One per 1/10 seconds and 180 degrees out of phase. Or simply a pulse every 50 ms. This serves as a good monitor, to assure both prism returns are received, and the laser is uniformly illuminating the airborne component input aperture.

RANGE

Range to the airborne component is measured using a commercial tellurometer. This device uses a near infrared output. This output beam retroreflects from the polarimeter polarization corner cube and is detected by the tellurometer detector. The distance is measured by amplitude modulation of the output and alternately switching the propagation path over a reference pathlength and the desired measured path. Several modulation frequencies are used and the two returns phase detected.

The most important aspect of this tellurometer is proper operation. A manual/auto switch is provided to achieve proper set up. Two levels must be set. The output signal level, first knob, and the reference level, second knob. The tellurometer must be switches on. The auto/manual switch is set to manual and the pushbutton switch depressed until the first LED light illuminates. The output level is adjusted to bring the meter level (received signal strength) to the green line, by adjusting the first knob (also off/on switch). The pushbutton is depressed a second time. The second knob is used to balance the reference path signal level, again by a green line reading. The instrument is now set up and used in the total range measurement position of the function switch (third knob). This is the first position to the right of the 8888.88 display test position. The auto/manual switch is returned to auto. Now the tellurometer will make ten measurements of range, average them, and provide a range display. Separate digital electronics lock in this measured range. The tellurometer display disappears between measurements, but the interface electronics store this range measurement, and update at each new measurement.

New data, programs, and outputs to the computer are accomplished using a standard teletype terminal. The actual PAM program is stored on floppy disc. (Also a data output recording disc.) A disc driver unit and disc provide the HP computer with the required memory.

4.0 COMPUTATION OF POSITION AND ATTITUDE

The PAM computer algorithm is provided with the six measurements made by the PAM components. These are azimuth, elevation, and magnitude (range) of the ground station vector to the airborne platforms; pitch, yaw, and roll angles of the airborne platform with respect to this location vector.

Azimuth and elevation are provided directly from the encoders on the tracking mount. Sixteen bit gray code outputs interface directly into the computer and are converted by the computer. Range comes directly from the tellurometer interface electronics to the computer. Four BCD digits are provided for range (i.e., 300.7 meters).

The pitch and yaw encoder data, as discussed previously, is processed and the corresponding pitch or yaw angle is locked into registers by the received returns. This data is interfaced to the computer by 16 bit binary. Roll is measured by the polarimeter. Its display is in degrees, and interface electronics process this angle into 16 bit binary and present it to the computer.

Since the data would under operational usage, be constantly changing, each measured quantity is stored in a 6 number push down stack. When the system is flashed the most recent and next two entries are used for each compilation. Each entry is scaled, and offsets introduced for processing. This raw data in addition to various error matrices are then used in the PAM algorithm to generate a position matrix of the airborne platform.

PRELIMINARY ALIGNMENT PROCEDURE

Airborne Component

The airborne component, AC was set up about 10 meters away from a vertical plywood screen in front of the GS HeNe laser. The laser illunimated the full aperture of the airborne component due to the use of an expanding lens.

The AC was oriented until the first surface reflection from the polarized corner cube returned on the laser. The pitch and yaw prims were then each covered by flat mirrors taped over the prism holders. Thus each mirror would sweep the laser reflection in a plane containing the laser and the perpendicular to the axis about which the mirror rotated (i.e., the shaft on which the prims are mounted). The theodolite mounted on a test fixture attached to the AC was then leveled and the tribrach adjustments sealed. The prism was rotated by hand and the top edge of the laser reflection observed on the plywood screen by the theodolite. The bearing purches were then adjusted until the laser reflection appeared to sweep a horizontal path. This insured the pitch prism shaft is perpendicular to a plane containing the vertical line (i.e., horizontal). Next the yaw prism shaft was rotated and the laser reflection from the mirror observed to sweep vertically. This insures that the shaft is perpendicular to a plane containing the horizontal line (i.e., vertical). Since the two shafts have intermeshing bevel gears, the two shafts can be considered to intersect at a point. This establishes the orthogonality of the shafts. As the theodolite was used to determine the horizontal and vertical. This procedure also establishes the parallelism of the AC yaw axis and the theodolite vertical axis. The flat mirrors covering the prisms were then removed and the prisms adjusted to sweep the respective laser reflections horizontally and vertically through the laser as seen on the plywood screen by the theodolite. This establishes the prisms to be aligned perpendicular to their respective shafts. Note that it is not possible to determine the offsets between the zero of the respective shaft angle encoder outputs and the true zero of the pitch or yaw of the AC. The reason for this is the spacial offset between the respective prisms and the effective

center of the AC coordinate system. A secondary reason for the inaccuracy of setting pitch/yaw offsets at close range is that the pitch/yaw receiver is a threshold device and would trigger on the leading edge of the reflection. At close range this could introduce significant error at operational distances. The time during which the reflection passes through the receiver is short enough to introduce negligible error. Also, as the reflection always sweeps through in the same direction the "leading edge effect" introduces negligible error.

Note also that the use of a beam expander lens in the laser introduces a different laser beam divergence. This combined with the effect of the physical separation between the center of the effective AC coordinate system and the polarized corner cube could also introduce significant error. The strong first surface reflection at close range could also introduce a significant error as the polarimeter would see the polarization component of the incoming laser beam confusing, in addition to that of the desired polarization due to the polaroid sheet in front of the corner cube.

Gimbal Mounted Sensors

A surrogate target was constructed on posterboard which consisted of circles equal in diameter to the aperture of the respective sensors and centered at just slightly less than the actual distances between the centers of the respective apertures. This provides a means of aligning the sensors to be slightly convergent and thus assuring that the sensors will all overlap on the airborne component. This target was set up vertically about 10 meters in front of the GS.

1. Polarimeter: A small test fixture bulb with a frosted gloss surface was substituted for the light pipe on the polarimeter to project a beam corresponding to its field of view. The surrogate target was positioned such that the projected beam (observed in a darkened room) was centered in its target circle.
2. Pitch/Yaw Receiver: This had been previously aligned to the polarimeter by a similar procedure where the receiver is illuminated by a chopped laser behind the center of the pitch/yaw receiver aperture on the target. The field of view of the receiver was then mechanically adjusted to center on the illuminating chipped laser.

3. Laser: The beam steering mirror of the laser/polarimeter pitch and yaw receiver assembly was adjusted to steer the laser beam to its target circle.

4. Laser (Pol/Ply) Assembly: After leveling the reference slate on the GS, the gimbal was then slewed such that the back surface of the main mounting plate was level. A shallow tray of water was then placed beneath the laser tilted such that the bottom reflection was off to the side and the reflection from the surface of the water was on the laser/pol/ply assembly. The assembly was then adjusted so as to bring this reflection directly back into the laser. The water acts as a self-leveling mirror and a retroreflection from the water surface is thus a true vertical. Since the reference plate has been aligned to be level when the main gimbal axis of the tracker is horizontal, this adjustment guarantees that the minor gimbal is pointed such that the laser beam is perpendicular to the major gimbal axis. (Note the design of the main mounting plate for the sensors is such that the back surface is parallel with the minor gimbal axis.)

5. Sighting Scope: The gimbal was then slewed so as to position the laser back on its target circle. The scope was then adjusted to center its crosshairs on the center of its target circle and rotated to align the crosshairs with vertical and horizontal marks on the target circle.

6. The tellurometer output beam was then observed using an IR viewer and adjusted to put its output spot on its target circle. The tellurometer receiver is adjusted during operation for max signal by a control on the tellurometer.

7. The TV camera was allowed to acquire and track its target circle center mark. The TV camera was then adjusted to bring the laser beam back on its target spot.

COORDINATE RELATIONSHIPS IN PAM

This section gives equations for converting measurements made in a coordinate system on board a remotely piloted vehicle (RPV) into ground-fixed coordinates by means of the information supplied by the Position and Attitude Monitor (PAM) now under design. The RPV is a comparatively quiescent airborne platform observed from the ground by the PAM at close range.

The PAM consists of a ground-based laser angle tracker that points itself at a cube-corner retroreflector mounted on the vehicle. Over the face of the cube corner is a sheet of Polaroid, which causes the retroreflected

laser beam to be linearly polarized, and the direction of this polarization as it arrives back at the ground is measured. By these means the angles a, b, and c of Figure 1 are obtained. On the vehicle are also two spinning roof prisms that return brief pulses of laser light to the receiver when they pass through certain positions in their rotation. Zero positions of the prisms (spinning about axes x and y in the vehicle) are telemetered to the ground, and in this way the angles d and e on board the RPV are obtained.

Rigorous definitions, and the equations for transforming coordinates x y z, measured with the respect to axes fixed in the vehicle, into the ground-based coordinates x_o y_o z_o follow. The PAM measures five angles, the positive sense in each case being taken as shown in Figure 4-1.

angle a between inner gimbal axis A-A and axis y_o,

angle b between outer gimbal axis x_o and plane P normal to the line of sight (LOS),

angle c between the E vector of the retroreflected light and a reference in plane P. (The reference chosen coincides with axis x_o when angle b is zero.),

angle d between the z axis and the projection of the LOS onto the y z plane, and

angle e between the z axis and the projection of the LOS onto the x z plane.

From these measured quantities the following additional entities, useful to the analysis and shown in Figure 4-1 are determined:

direction cosines ℓ, m, n of the LOS in the airborne (x y z) coordinate system,

angle θ between the LOS and axis z. (Axis z is normal to the Polaroid, which is oriented so that its E-pass direction is along axis x. Therefore θ is the angle of incidence of the LOS with the Polaroid, and plane LOS-z is the plane of incidence.),

angle ψ between the plane of incidence and plane x z, and

angle ω between the E vector of the retroreflected light and the plane of incidence. This angle lies in plane P because E lies in plane P.

The relation between coordinates x y z of a point (direction) measured in the airborne system and the coordinates of x_o y_o z_o of the same point in

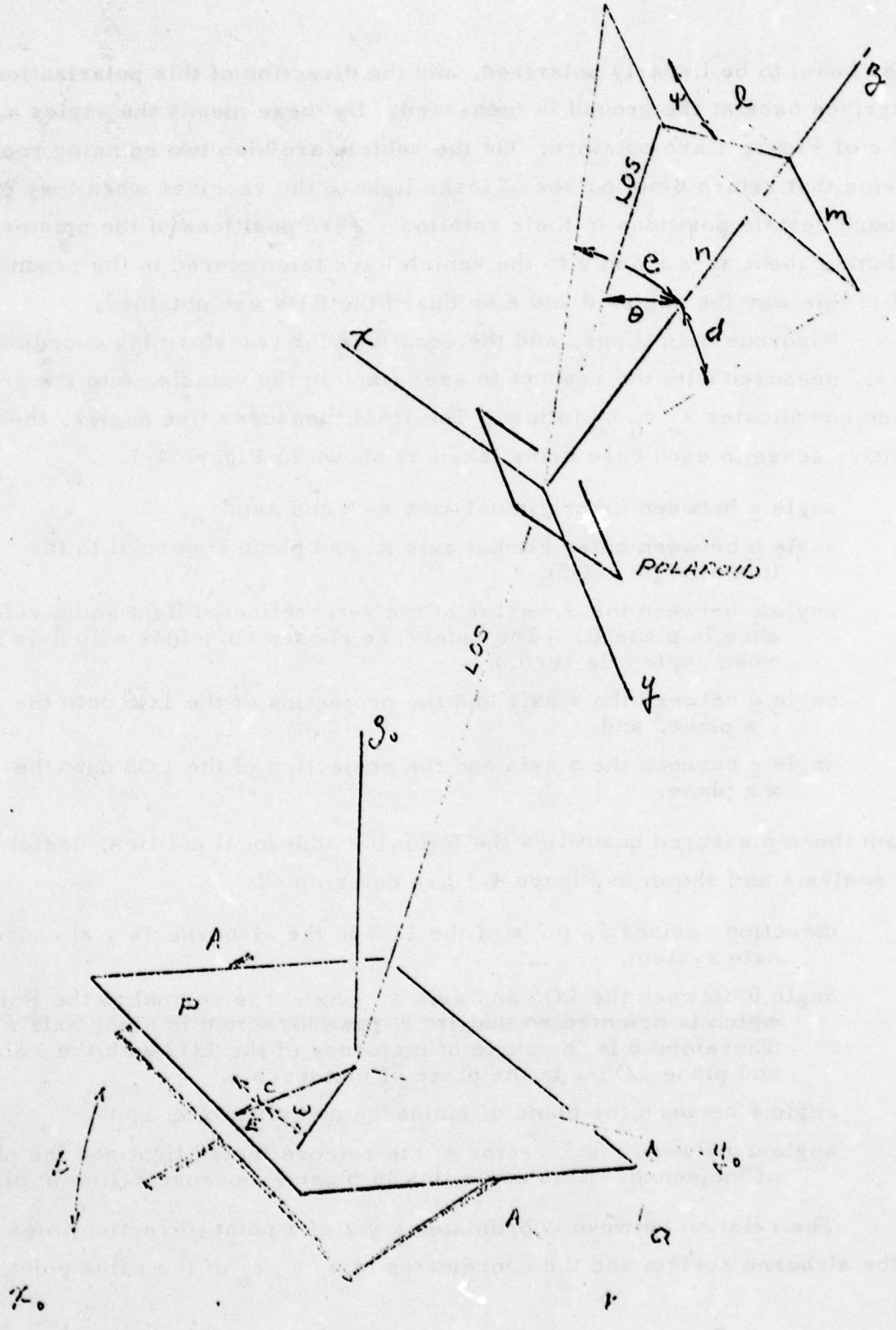

Figure 4-1.

the ground system (both systems orthogonal right handed) is, of course, simply a rotation of axes.

$$\begin{matrix} x_o \\ y_o \\ z_o \end{matrix} = [R] \begin{matrix} x \\ y \\ z \end{matrix} . \qquad (1)$$

Here R is a 3 x 3 rotation matrix, which may be conveniently written as a product of simpler matrices that separate the various parameters defining the overall rotation. Thus

$$R = R_1 R_2 R_3 R_4 R_5 \qquad (2)$$

where

$$R_1 = \begin{bmatrix} 1 & 0 & 0 \\ 0 & \cos a & \sin a \\ 0 & -\sin a & \cos a \end{bmatrix} , \quad R_2 = \begin{bmatrix} \cos b & 0 & -\sin b \\ 0 & 1 & 0 \\ \sin b & 0 & \cos b \end{bmatrix}$$

$$R_3 = \begin{bmatrix} \cos(c+\omega) & -\sin(c+\omega) & 0 \\ \sin(c+\omega) & \cos(c+\omega) & 0 \\ 0 & 0 & 1 \end{bmatrix} ,$$

$$R_4 = \begin{bmatrix} \cos\theta & 0 & -\sin\theta \\ 0 & 1 & 0 \\ \sin & 0 & \cos\theta \end{bmatrix} , \quad R_5 = \begin{bmatrix} \cos\psi & \sin\psi & 0 \\ -\sin\psi & \cos\psi & 0 \\ 0 & 0 & 1 \end{bmatrix} .$$

Matrices R_1 and R_2 involve only the directly-measured angles a and b, and so need no further discussion, but R_3, R_4, and R_5 contain quantities not yet explicitly given. We note from Figure 4-1 that

and

$$\begin{aligned} m &= -n \tan d \\ \ell &= n \tan e \end{aligned} \qquad (3)$$

from which, because $\ell^2 + m^2 + n^2 = 1$, we get

$$n = (\tan^2 d + \tan^2 e + 1)^{-1/2} = \cos \theta. \tag{4}$$

We also have

$$\tan \psi = m/\ell, \tag{5}$$

so apparently we can compute R_4 and R_5. Equation (4) is not much good as-is for finding θ because 0 is a small angle ($0 < 0 < 20°$) whose cosine is near one. However, we also have

$$\sin^2 0 = \ell^2 + m^2 \quad , \tag{6}$$

so this presents no problem. Equation (5) will cause trouble because both ℓ and m may be zero; this will be considered later in this memorandum.

Calculation of R_3 requires the value of ω, the angle between the electric vector of the light wave retroreflected along the LOS and the plane of incidence. This angle depends upon the way in which a plane wave of light that has been linearly polarized inside a sheet of Polaroid material is reflected and refracted upon leaving the sheet. This matter does not seem to have been discussed in any depth in the literature, but the paper by Baxter[1] makes some unsubstantiated statements about it. Polaroid is a uniaxial optical medium in which the extraordinary ray is strongly attenuated, leaving only the linearly-polarized ordinary ray. If we assume that this ordinary wave, upon leaving the sheet, acts the same at the Polaroid-air interface as it would in leaving an isotropic medium of index μ, then we have for the refracted wave

$$2E_{\parallel} = 1E_{\parallel} \frac{2}{\frac{\cos \theta_2}{\cos \theta_1} + \frac{\mu_2}{\mu_1}} \quad ; \quad 2E_{\perp} = 1E_{\perp} \frac{2}{1 + \frac{\mu_2 \cos \theta_2}{\mu_1 \cos \theta_1}} \tag{7}$$

In these equations ${}_1E$ is the total electric field of the light wave internally incident on the interface, ${}_2E$ is the total electric field of the refracted wave, $\parallel$ and $\perp$ mean the components polarized parallel and perpendicular to the plane of incidence, and subscripts 1 and 2 on μ and θ identify medium 1 (the Polaroid) and medium 2 (air).

These equations give:

$$\tan \omega = F(\theta) * \tan \psi \tag{8}$$

where

$$F(\theta) = \frac{\cos \theta + \frac{1}{\mu^2}\sqrt{\mu^2 - \sin^2 \theta}}{1 + \frac{\cos \theta}{\sqrt{\mu^2 - \sin^2 \theta}}} \tag{9}$$

Equation (8) defines the familiar S-curve, encountered frequently in physical problems; it is shown in Figure 4-2.

Note that $\omega = \psi$ whenever ψ is an integral multiple of 90°, and that between these values $\omega - \psi$ oscillates with an amplitude that increases with the departure of F from unity.

If $\mu = 1.5$ and $\theta < 20°$ then $0.96 < F(\theta) < 1$, in which case ω never departs from ψ by so much as one degree, even though ψ may lie anywhere in the four quadrants. For this reason, as well as because of the fact that the plane of incidence, from which ω and ψ are measured, is ill-defined when θ is small and is indeterminate when θ is zero (the center of PAM's nominal range), it would seem desirable to work directly with $\omega - \psi$. This can be accomplished by operating on the last three matrices of (2) as follows:

$$R_3 R_4 R_5 = R_3 R_5 * R_5^{-1} R_4 R_5 = R_6 * R_7 \quad , \tag{10}$$

$$\tan \omega = F * \tan \psi$$

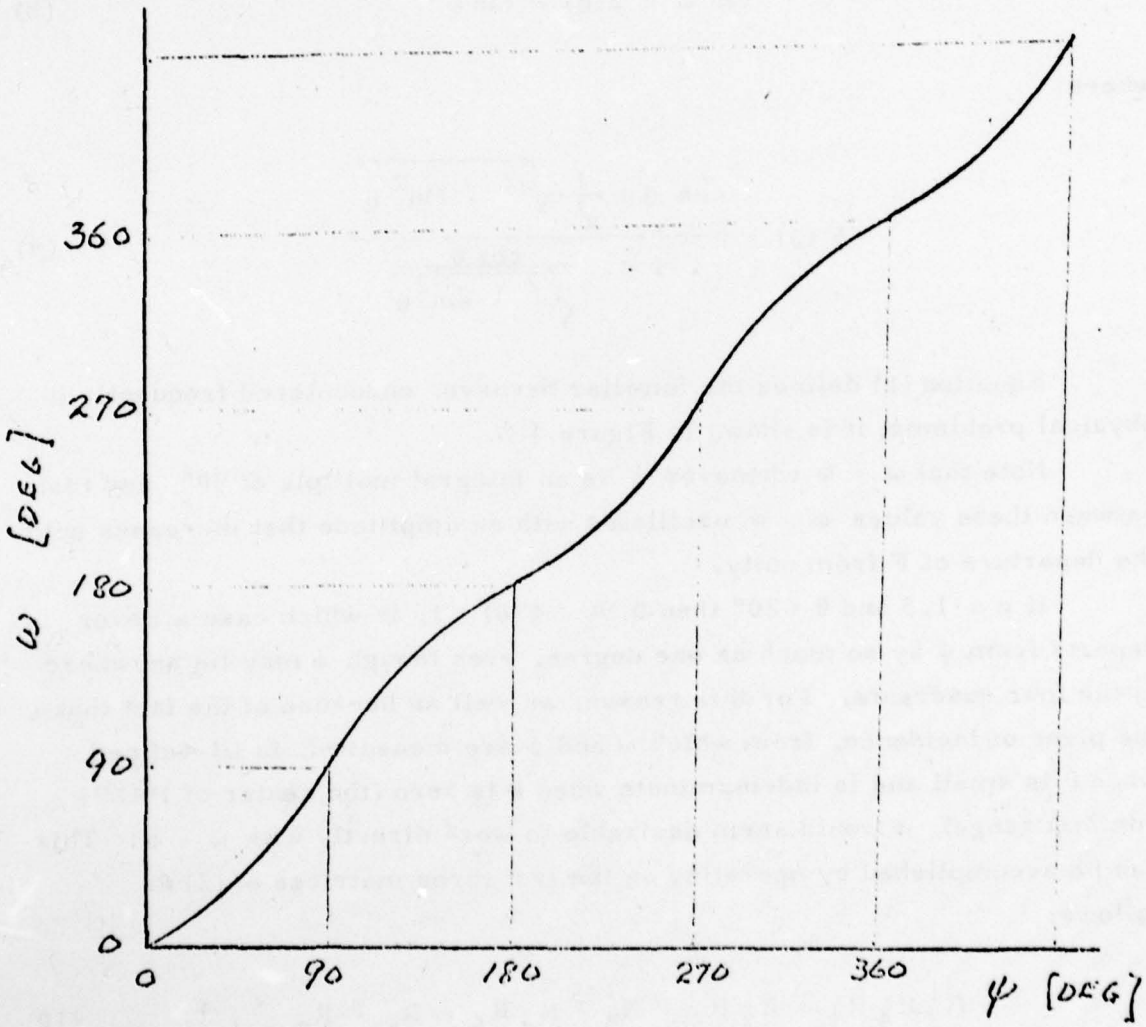

Figure 4-2.

which when multiplied out gives

$$R_6 = \begin{bmatrix} \cos(c + \omega - \psi) & -\sin(c + \omega - \psi) & 0 \\ \sin(c + \omega - \psi) & \cos(c + \omega - \psi) & 0 \\ 0 & 0 & 1 \end{bmatrix} \tag{11}$$

and

$$R_7 = \begin{bmatrix} 1 - \frac{\ell^2}{n+1} & -\frac{\ell m}{n+1} & -\ell \\ -\frac{\ell m}{n+1} & 1 - \frac{m^2}{n+1} & -m \\ \ell & m & n \end{bmatrix} \tag{12}$$

Notice that R_7 is well behaved; ℓ and m are less than one (in fact relatively small compared to one) and n is near unity.

R_6 requires that we compute $\omega - \psi$, and (8) can be put into various forms that facilitate this; one straightforward procedure goes as follows:

$$\tan(\psi - \omega) = \frac{(1 - F)\tan\psi}{1 + F\tan^2\psi} = \ell m f (1 - fm^2)^{-1}, \tag{13}$$

where the third form comes from putting in m/ℓ for $\tan\psi$ and defining f

$$f \equiv \frac{1 - F}{\ell^2 + m^2} \tag{14}$$

A computer will still have trouble when $\theta = 0$ ($\ell = m = 0$), but this is now easily fixed. Physically there is no problem; if $\theta = 0$ then $F = 1$ and $\omega = \psi$ from (8). Expanding F as a function of $\sin\theta$ ($\equiv s$)

$$F(\theta) = 1 - c_1 s^2 - c_2 s^4 - c_3 s^6 - c_4 s^8 \ldots\ldots \tag{15}$$

where, after some algebra, we find that

$$c_1 = \frac{\mu^2 - 2\mu + 2}{2\mu^2} \quad (= 5/18)$$

$$c_2 = \frac{\mu^3 - 4\mu + 4}{8\mu^3} \quad (= 11/216)$$

$$c_3 = \frac{\mu^5 - 2\mu^3 + 2}{16\mu^5} \quad (= 91/3888) \qquad (16)$$

$$c_4 = \frac{5\mu^7 - 8\mu^5 + 8}{128\mu^7} \quad (= 4183/279936)$$

(The numbers in parenthesis correspond to $\mu = 3/2$)

From (13), (14), and (15) we now have

$$\tan(\psi - \omega) = \ell m f (1 + f m^2 + f^2 m^4 + f^3 m^6 \ldots\ldots)$$

with

$$f = c_1 + c_2 s^2 + c_3 s^4 + c_4 s^6 + \ldots\ldots,$$

and if we also make use of

$$\tan^{-1} x = x - \frac{x^3}{3} + \ldots\ldots$$

after more algebra, we arrive at

$$\psi - \omega = \ell m (A_0 + A_1 \ell^2 + A_2 m^2 + A_3 \ell^4 + A_4 \ell^2 m^2 + A_5 m^4 + A_6 \ell^6 + A_7 \ell^4 m^2 + A_8 \ell^2 m^4 + A_9 m^6 \ldots), \qquad (17)$$

where the As are functions of the cs:

$$A_0 = c_1 \qquad (0.27777778)$$

$$A_1 = c_2 \qquad (0.05092593)$$

$$A_2 = c_1^2 + c_2 \qquad (0.12808642)$$

$$A_3 = c_3 \qquad (0.02340535)$$

$$A_4 = -\frac{1}{3} c_1^3 + 2 c_1 c_2 + 2 c_3 \qquad (0.06795839)$$

$$A_5 = c_1^3 + 2 c_1 c_2 + c_3 \qquad (0.07313100)$$

$$A_6 = c_4 \qquad (0.01494270)$$

$$A_7 = c_1^2 c_2 + 2 c_1 c_3 + c_2^2 + 3 c_4 \qquad (0.05649506)$$

$$A_8 = -c_1^4 + 2 c_1^2 c_2 + 4 c_1 c_3 + 2 c_2^2 + 3 c_4 \qquad (0.07792615)$$

$$A_9 = c_1^4 + 3 c_1^2 c_2 + 2 c_1 c_3 + c_2^2 + c_4 \qquad (0.04828127)$$

Equation (17) looks as bad as (8) and (9) where we started, but a computer will do much better with (17), because the As are all positive constants, and no divisions or subtractions occur to cause overflow or round-off problems. Also the number of arithmetic operations will be much smaller than would be involved in computing the trigonometric functions of (8) and (9).

As a numerical check on the validity of this expansion we note that (17) is exact when either ℓ or m are zero — then $\omega = \psi$, as concluded originally from (8). The greatest error will occur when ℓ and m are about equal in size. In that case $\ell^2 = m^2 = \frac{1}{2} s^2$ and (17) becomes

$$\psi - \omega = (5/36)\, s^2 + 0.04475309\, s^4 + 0.02056184\, s^6 + 0.0123528\, s^8 . \qquad (18)$$

Table 4-1 and Figure 4-3 show the differences between the values of $\omega - \psi$ computed from (8) and (9) and the corresponding values computed from (18) for different values of θ. The four monotonic curves correspond to truncating (18) after terms in s^2, s^4, s^6, and s^8. We note from these data that for $0 < \theta < 20°$, using only terms through 4th degree would probably be adequate.

Equation (17) is an ordinary Taylor power series in ℓ and m; it could be economized to a Chebyshev series with considerable reduction in the computing required, but the effort of writing this out here does not seem justified until some experimental laboratory data on the degree of applicability of (8) and (9) to real Polaroid are obtained. Baxter's paper[1] says without derivation that (in our notation) "$\omega - \psi \simeq B\,\theta^2 \sin 2\psi$ when θ is small." His B is the same as my $-c_1/2$, which indicates that he makes the same assumption I have made that the ordinary wave leaves the Polaroid as it would an isotropic medium. I am not sure that this assumption is right; in any case any optical coating, intentional or otherwise on the Polaroid exit face will alter things, so this must be looked into in the laboratory.

Physically it is apparent that for any particular equipment condition $\omega - \psi$ will be <u>some</u> function of ℓ and m, and it may turn out that the most efficient computer program will come from determining this function empirically and the then Chebyshev expanding. An an example of the type of error curve to be expected, Figure 4-3 includes a curve obtained by converting (18) to a sum of Chebyshev Polynominals $T_k^*(x)$, where $x = (s/\sin 20°)^2$, and then discarding everything beyond $T_2^*(x)$. This is equivalent to using

$$\psi - \omega = 0.000001155 + 0.13871332\, s^2 + 0.0486568\, s^4 \qquad (19)$$

for the approximating function. Notice that for $0 < \theta < 20°$ the maximum error is not much more than one microradian, whereas the Taylor series through s^4 has an error of about 35 μrad at $\theta = 20°$.

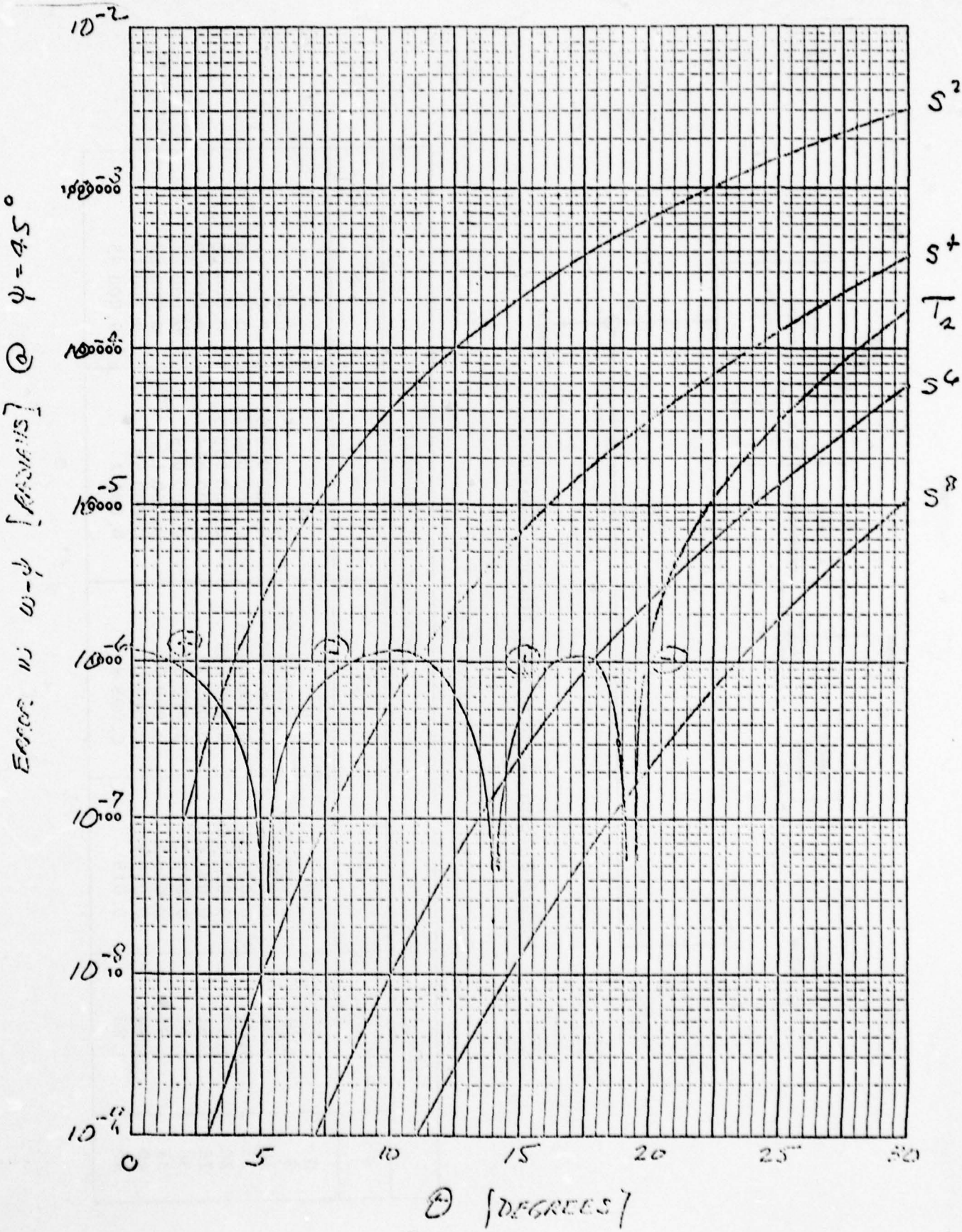
ERROR IN Ω-ψ [RADIANS] @ ψ = 45°
10^-2
10^-3
10^-4
10^-5
10^-6
10^-7
10^-8
10^-9
0
5
10
15
20
25
30
θ [DEGREES]
S^2
S^4
S^6
S^8
T/2

Figure 4-3.

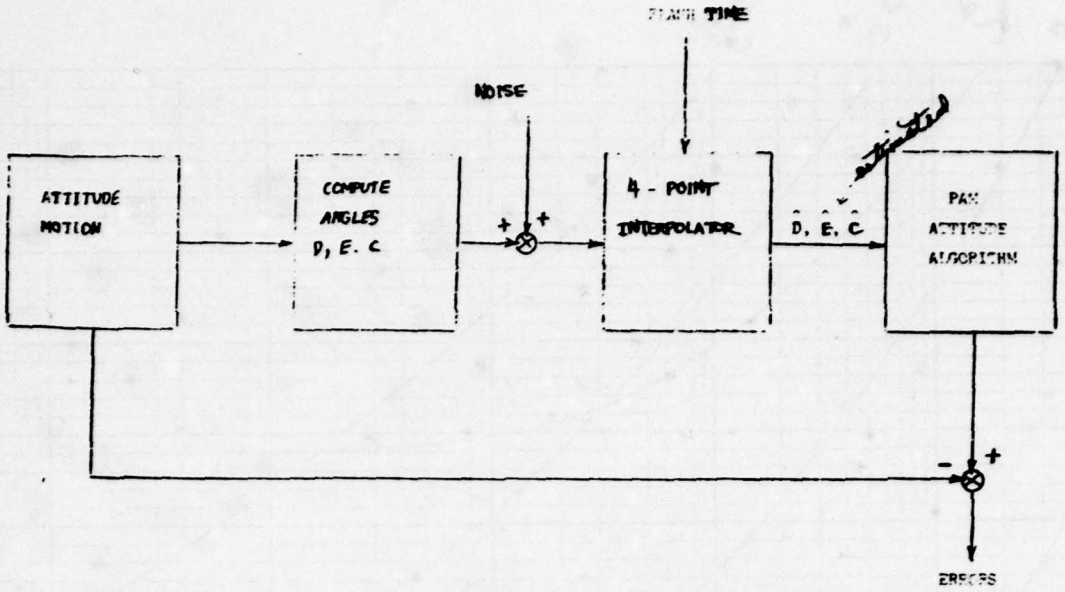

Figure 6. Simulation of PAM Attitude Algorithm

TABLE 4-1

[Deg]		$\omega - \psi$ Error in [Radians]			
θ	$\lvert\omega-\psi\rvert_{max}$	S^2	S^4	S^6	S^8
0	0	0	0	0	0
5	0.06	0.000 0026	0.000 000 01	0.0	0.0
10	0.24	0.000 041	0.000 000 57	0.000 000 01	0.0
15	0.54	0.000 21	0.000 006 4	0.000 000 26	0.000 000 013
20	0.97	0.000 65	0.000 035	0.000 002 5	0.000 000 21
25	1.51	0.001 6	0.000 13	0.000 014	0.000 001 9
30	2.17	0.003 2	0.000 38	0.000 059	0.000 011
35	2.95	0.005 8	0.000 92	0.000 19	0.000 046
40	3.84	0.009 6	0.002 0	0.000 52	0.000 16
45	4.84	0.015	0.003 8	0.001 2	0.000 45

SIMULATION OF PAM ATTITUDE ALGORITHM

Summary

The PAM determines the attitude of the RPV given the measured values of five angles. Three angles are measured with optical techniques, two are conventional gimbal angles.

The algorithm described above per se, is exact (with the assumptions on the propagation through the polaroid). The purpose of the simulation then was to study the effect of various system parameters and error sources on this algorithm. The principal features investigated were sampling rate, i.e., prism rotational frequency, measurement noise and variation of the polaroid index of refraction from its nominal value. Other effects considered were quantization of the measurement and flash times, and phasing of the roll measurement.

For studying all of these effects, the RPV motion was assumed to be a 3-dimensional sinusoid with 2 deg. amplitude at a 1 Hz frequency. The last part of the study considers a transient motion wherein the motion of the RPV is the output of a triangular pulse through a low-pass filter.

The principal conclusion of the investigation is that for the 2 deg., 1 Hz sinusoidal motion the accuracy requirement of 0.25 mr for determining RPV attitude can be satisfied with a prism frequency of 5- 8 Hz using a 6 or possibly an 8-point interpolator, provided that the optical measurement errors are limited to about ±0.1 mr and the polaroid uncertainty is limited to about ±1% of nominal value.

The simulation was solved on the DEC-10 time-share system. Programming and running of the problem was performed by Jeff Wagner.

Simulation Overview

A block diagram of the simulation is given in Figure 4-4. The attitude motion was prescribed in terms of the Euler axis and angle, as described in Reference 3. It is shown there that the nine components of a direction cosine matrix which relate a moving frame and a fixed frame can be conviently expressed in terms of a single axis and angle. The direction cosines

TABLE 4-2. TABLE OF SYMBOLS

ℓ_E, m_E, n_E	direction cosines of the vehicle (RPV) axis of rotation
θ	vehicle rotation angle around this axis, $= A \sin(w_V t) + \phi_V$, for sinusoidal motion
A	amplitude (degs.)
w_V	vehicle frequency (rad/sec)
t	time
ϕ_V	average offset angle for θ, (degs)
f_p	prism frequency (Hz)
μ, μ	actual and assumed polaroid index of refraction
D, E, C	pitch, yaw and roll angles, respectively
E_X, E_Y, E_Z	error angle between the true and estimated attitudes of the vehicle x, y, z axes (mr)
E_a	average error angle, $= 1/3 (E_X+E_Y+E_Z)$
t_f	flash time (secs)
Q	quantization level
t_Q	quantized time
T	period of the triangular pulse
τ	time constant of low-pass filter used with triangular motion, $= (1/2\pi)$ secs.

of this axis with respect to the fixed ground axes are designated herein as ℓ_E, m_E, n_E and the angle by θ. The former are constants on any one run, whereas θ is a function of time, viz, sinusoidal or a triangular pulse through a low-pass filter. For simplicity, and with no loss of generality, the line-of-sight (LOS) from the PAM ground component to the airborne component was assumed to be vertical. This made the two mechanical gimbal angles zero. A large angle (~20 degs) between the LOS and the RPV z axis (perpendicular to the polaroid plane) was still obtained by choosing $\phi_V = \pm 25$ degs. (see Table of Symbols).

Computation of the pitch and yaw angles D, E was the most difficult part of the simulation as it involved solution of a transcendental equation for determining the retroreflection times. Computation of the roll angle C was more straightforward although not trivial. Details of these computations are not given in this report.

Since the data times are not synchronous with the flash time, interpolators are required to obtain the values of pitch, yaw and roll angles at the flash time. Three 4-point interpolators (one for each channel) were used in the simulation such that two data points lay on each side of the assumed flash time. 6 and 8 point interpolators with 3 and 4 data points, respectively, on each side of the flash time have been studied separately apart from the simulation. In general, it was found that the errors obtained from the simulation using the 4-point interpolator were in good agreement with the hand-calculated errors. Thus, it was considered unnecessary to alter the simulation to include the 6 or 8-point interpolators, since their errors could be estimated from hand calculations. The general n-point interpolator is discussed in the Appendix.

The interpolators are the estimated values of the pitch, yaw and roll measurements at the flash times, viz $\hat{D}$, $\hat{E}$, $\hat{C}$. These are then inputted to the PAM attitude algorithm as described in Reference 2 (with some negligible differences, involving expansion of an inverse tangent). The estimated attitude of the RPV as determined by the algorithm is then compared to the exact attitude. Errors E_x, E_y, E_z between the exact and estimated attitudes of the RPV x, y, z axes are computed. Also computed is the average error. These are the principal outputs when examining the effects of any system parameter or error source.

Results

The parameters and error sources examined were:

1. Phasing of the roll measurement
2. Rotational frequency of the prism
3. Measurement noise
4. Uncertainty in the polaroid index of refraction

5. Quantization of measurement and flash times

6. Filtered "triangular" vehicle motion replacing sinusoidal motion

For studying effects 1. - 5. the RPV motion was a 3-axis sinusoidal motion. The direction cosines of the Euler axis with respect to the local vertical ground coordinate frame were

$$\ell_E = m_E = n_E = 1/\sqrt{3}$$

Angle θ was

$$\theta = (3.5 \text{ deg}) \sin (2\pi t) + \phi_v$$

Observe that

$$3.5 \text{ deg} \times (1/\sqrt{3}) = 2 \text{ deg along each axis*.}$$

As seen, the vehicle frequency was

$$w_v = 1 \text{ Hz} = 2\pi \text{ rad/sec}$$

The offset angle ϕ_v was chosen as 25 deg or -25 deg. It can be shown that with $n_E = 1/\sqrt{3}$, choosing $\phi_v = 25$ deg makes the average angle between the LOS (which was vertical) and the RPV z axis (perpendicular to the polaroid) approximately 20.4 deg.

The flash time was chosen as $t_{f\ell} = 0.75$ sec. Thus, $2\pi t_{f\ell} = 3\pi/2$ which, according to the discussion in the Appendix on interpolators, produces worst case errors for the interpolators.

---

*This is approximately true since the angles are small. Finite angles, of course, cannot be treated as vectors.

Early in the simulation study it was thought that the roll measurements would be available at some rate greater than the prism frequency; a roll data rate of twice the prism frequency was then assumed as a reasonable value. The two roll measurements were conveniently assumed to be available when the normals to the pitch and yaw prism faces were parallel to the vehicle z axis. Later, it was learned that the roll measurements would be available only once per prism rotation, but their phasing was still unspecified. It was decided therefore to study parametrically the effects of phasing of the roll measurement relative to pitch and yaw.

The 3-axis sinusoidal motion with ϕ_v = 25 degs was used. The prism frequency f_p was chosen as 12 Hz. The roll measurement was made once/cycle of the prism rotation and the phasing was varied in steps of 30 degs starting from 0, where 0 means the roll measurement occurs when the normal to the x-axis prism is aligned with the -z vehicle axis. There were no other system errors.

The attitude errors E_x, E_y, E_z, E_a are shown in Table 4-2 as a function of the phasing.

TABLE 4-2. EFFECT OF PHASING OF ROLL MEASUREMENT

Phase, degrees	E_x, mrad	E_y, mrad	E_z, mrad	E_a, mrad
0	0.05	0.01	0.05	0.04
30	0.06	0.01	0.06	0.04
60	0.06	0.03	0.06	0.05
90	0.07	0.04	0.06	0.06
120	0.08	0.04	0.06	0.06
150	0.08	0.05	0.07	0.07
180	0.08	0.05	0.07	0.07
210	0.08	0.05	0.07	0.07
240	0.08	0.05	0.06	0.06
270	0.07	0.04	0.06	0.06
300	0.06	0.03	0.06	0.05
330	0.06	0.01	0.06	0.04

These results show that the phase of the roll measurement has a small effect on system accuracy, at least for f_p = 12 Hz with the 4-point interpolator. At a lower frequency such as 10 Hz, the differences in the errors would probably be larger. However, since the intention is to choose a combination of f_p and the interpolator order such that errors due only to interpolation are typically no greater than those in Table 4-2, any phasing of the roll measurement at the prism frequency should be acceptable.

The second group of runs shows the effect of varying both the prism frequency and the initial offset angle. The roll measurement had a phasing of 180 degs., this always giving worst case errors as shown in Table 4-2. Results of the second group of runs are shown in Table 4-3.

The effect of prism frequency is nicely illustrated by the first three runs. It is seen that the average error decreases from 0.1 to 0.07 to 0.02 mrad as f_p increases from 10 to 12 to 15 Hz. These errors are in good agreement with hand calculations for the maximum errors of an equispaced 4-point interpolator with an input of 2 deg sine wave at 1 Hz, these errors being 0.12, 0.06 and 0.02 mr, respectively (see Appendix). For ϕ_v = -25 degs (which gives the same average angle of incidence of 20.4 degs as ϕ_v = 25 degs) the average errors are 0.07, 0.08 and 0.03 mr for f_p = 10, 12, 15 Hz, respectively. While these results are somewhat erratic, there is nothing particularly detrimental about them. An explanation for the lower-than-expected error at f_p = 10 Hz is that, in this case, the flash time occurs very close to one of the data times.

TABLE 4-3. EFFECT OF PRISM FREQUENCY AND OFFSET ANGLE

ϕ_v, degrees	f_p, Hz	E_x, mrad	E_y, mrad	E_z, mrad	E_a, mrad
25	10	0.02	0.14	0.14	0.10
25	12	0.08	0.05	0.07	0.07
25	15	0.03	0.02	0.02	0.02
-25	10	0.04	0.08	0.08	0.07
-25	12	0.10	0.07	0.07	0.08
-25	15	0.03	0.02	0.03	0.03

The third group of runs shows the effect of measurement noise. Bias errors of plus or minus 0.05 mr were assumed on the pitch, yaw and roll measurements. Four combinations of errors were selected. The prism frequency was 12 Hz, the phase angle for the roll measurement was 180 degs and ϕ_v was 25 degs. Results are shown in Table 4-4.

The RSS error of the three noise errors and the average error from the interpolator of 0.07 mr (from Table 4-3)is

$$RSS = \left[3 \times (0.05)^2 + (0.07)^2\right]^{1/2} = 0.11 \text{ mr}$$

which is the same as the average of the four values of E_a, i.e.,

$$(0.09 + 0.14 + 0.09 + 0.13)/4 = 0.11 \text{ mr}$$

Using RSS calculations, the measurement errors could be doubled to ±0.1 mr and still satisfy the 0.25 mr spec. In this case, the RSS value is

$$RSS = \left[3 \times (0.1)^2 + (0.07)^2\right]^{1/2} = 0.19 \text{ mr}$$

The fourth group of runs shows the effect of uncertainty in μ, the polaroid index of refraction. μ is a parameter in the PAM attitude algorithm so that if there is a mismatch between the assumed and actual values of μ, this can produce an error. Currently, the nominal value of μ is 1.5. In

TABLE 4-4. EFFECT OF MEASUREMENT NOISE

E_D mrad	E_E mrad	E_C mrad	E_x mrad	E_y mrad	E_z mrad	E_a mrad
0.05	0.05	0.05	0.10	0.11	0.07	0.09
0.05	-0.05	0.05	0.16	0.11	0.14	0.14
-0.05	0.05	0.05	0.11	0.12	0.05	0.09
-0.05	-0.05	0.05	0.16	0.11	0.13	0.13

the simulation, $\mu = 1.5$ was used in the PAM algorithm, while the true μ was varied by ±1% and ±2%. Again f_p was 12 Hz, phase angle for the roll measurement was 180 degs and ϕ_v was 25 degs. Results are shown in Table 4-5.

The ±2 percent variation, third and fourth cases, are somewhat unrealistic but are included for completeness. ±1 percent is probably a more reasonable maximum. The worst reasonable case errors occur for +1 percent, $\mu = 1.515$, producing an average error of 0.14 mr, the same as the worst case noise error of Table 4-4.

The next effect studied was quantization of the measurement and flash times. It was though this might be important because of the structure of the interpolators, which requires time differences between the measurement times, and the measurement times and flash time.

The algorithm for quantizing time is

$$t_Q = Q\ [\text{AINT}\ (t/Q)]$$

where

t_Q = quantized time
Q = quantization level
t = true value of time

AINT is a function which gives the largest integer of the real number (t/Q), e.g.:

AINT (15.0000) = 15.
AINT (15.0001) = 15.
AINT (15.9999) = 15.

TABLE 4-5. EFFECT OF UNCERTAINTY IN THE POLAROID INDEX OF REFRACTION

μ	E_x	E_y	E_z	E_a
1.515	0.17	0.15	0.09	0.14
1.485	0.06	0.05	0.04	0.05
1.53	0.26	0.24	0.12	0.20
1.47	0.15	0.16	0.04	0.12

A series of runs were made keeping all parameters fixed while varying Q. The standard 3-axis sinusoidal rotation was chosen. Other fixed parameters were f_p = 10 Hz, ϕ_v = 25 degs. All measurement errors were zero, μ, $\hat{\mu}$ had their nominal values of 1.5, and the phase angle of the roll measurement was zero.

The finish tire had two values:

$$t_{f\ell} = 0.75 \pm 0.000001 \text{ secs}$$

the purpose being to see whether quantization of the flash time would produce different results, even though for practical purposes the flash times were the same.

The results are shown in Table 4-6.

It is seen that the time quantization parameter Q has virtually no effect on the results, even for Q as large as 1000 μsec. Currently, the PAM computer Q is planned as approximately 100 μsec. If this leads to any timing problems which could be alleviated by using a larger Q, then these results show that Q can be increased considerably with no detrimental effects.

The last effect studied was a transient-type motion, which can be described as a filtered triangular motion. In this case, angle θ is taken as the output of a low-pass filter (time constant = $(1/2\pi)$ secs), whose input is a triangular pulse. This is sketched in Figure 4-5.

Using the symbols in Figure 4-5, it can be shown that output θ(t) is

$$\theta(t) = \frac{2A}{T}\left[\tau e^{-t/\tau} + t - \tau\right], \qquad 0 \le t \le T/2$$

$$= \frac{2A}{T}\left[\tau(1 - 2e^{T/2\tau})e^{-t/\tau} + T + \tau - t\right], \quad T/2 \le t \le T$$

At $t = T/2$, θ, $\dot{\theta}$ are continuous but $\ddot{\theta}$ and all its higher derivatives are discontinuous. Choosing T/2 as the flash time $t_{f\ell}$ and then equi-spacing the data points around $t_{f\ell}$ in at least one data channel should give a worst case.

TABLE 4-6. EFFECTS OF THE QUANTIZATION

$t_{f\ell}$ seconds	Q, μs	$E_{x'}$ mrad	$E_{y'}$ mrad	$E_{z'}$ mrad	$E_{a'}$ mrad
0.749999	0	0.12	0.17	0.13	0.14
0.749999	100	0.12	0.17	0.13	0.14
0.749999	200	0.12	0.18	0.12	0.14
0.749999	500	0.13	0.18	0.13	0.14
0.749999	1000	0.13	0.18	0.13	0.14
0.750001	0	0.12	0.17	0.13	0.14
0.750001	100	0.12	0.17	0.13	0.14
0.750001	200	0.12	0.18	0.13	0.14
0.750001	500	0.13	0.18	0.13	0.14
0.750001	1000	0.13	0.18	0.13	0.14

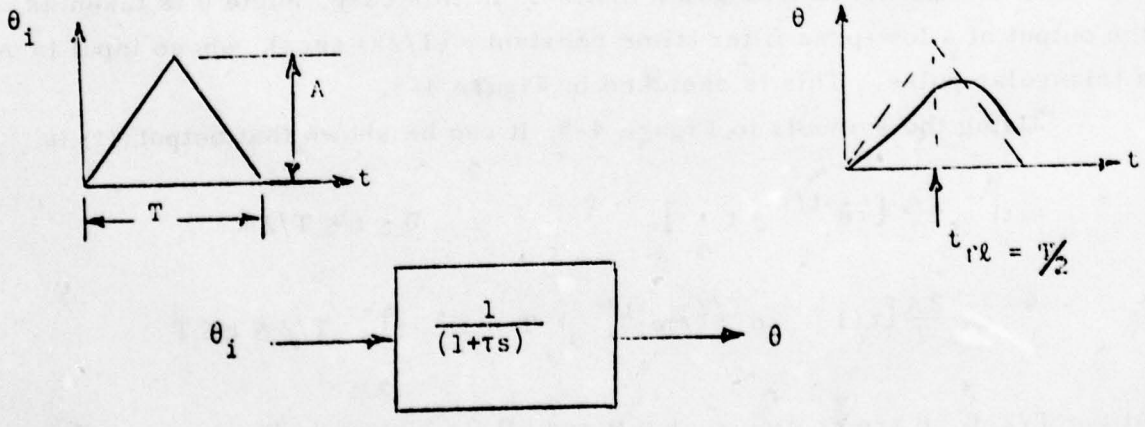

Figure 4-5. Triangular Pulse Input to Low Pass Filter

Amplitude A was 5 degs, pulse period was about 1 sec (to obtain worst case results, the exact value was made slightly dependent on f_p) and $\tau = (1/2\tau)$ secs. The usual 3-axis motion was used. To obtain 5 degs along each axis, the total amplitude was $5\sqrt{3} = 8.66$ degs. The offset angle ϕ_v was both 25 and -25 degs. Results are shown in Table 4-7.

The four cases with $f_p = 12$ Hz were actually run first with the two phase values of 0 and 180 degs, to see which gave the worst case. It is seen that for both $\phi_v = 25$ and -25 degs the errors are larger with phase = 0. (This is opposite to what was found with sinusoidal motion.) Thus when testing $f_p = 10$ and 15 Hz, only phase = 0 was used.

Comparing Tables 4-3 and 4-7 for $f_p = 10$, 12, 15 Hz, the worst case errors for this filtered triangular motion are two to four times greater than worst case errors for the 2 deg sinusoidal motion. Of course, this comparison is akin to the "apples vs oranges" comparison. The results in Table 7 are essentially worst, worst case results, e.g., if period T were increased (T can be as large as 5 secs) the errors would be considerably smaller.

Conclusions

A simulation was developed to study the effect of system parameters and error sources on the PAM attitude algorithm developed above. The three most significant effects were found to be:

- Prism frequency
- Measurement noise
- Variation in the polaroid index of refraction

Two other effects studied – phasing of the roll measurement and quantization of the measurement and flash times – were found to have little effect on system accuracy.

Considering only the first three effects and neglecting any other error sources, the PAM error requirement of 0.25 mr can be satisfied with a prism frequency of 5-8 Hz provided a 6 or 8 point interpolator is used (the lower frequencies requiring the higher order interpolator). Concomitantly, the measurement errors on the pitch, yaw and roll optical angles

TABLE 4-7. RESULTS OF 3-AXIS FILTERED TRIANGULAR MOTION

ϕ_v, (degrees)	Phase, (degrees)	f_p, (Hz)	T, (seconds)	E_x, (mrad)	E_y, (mrad)	E_z, (mrad)	E_a, (mrad)
25	0	10	1.1	0.27	0.22	0.19	0.23
25	0	12	1.083	0.17	0.13	0.12	0.14
25	180	12	1.083	0.08	0.07	0.10	0.08
25	0	15	1.0	0.11	0.07	0.08	0.09
-25	0	10	1.1	0.25	0.34	0.30	0.30
-25	0	12	1.083	0.16	0.21	0.19	0.19
-25	180	12	0.083	0.07	0.14	0.15	0.12
-25	0	15	1.0	0.10	0.13	0.12	0.12

should be limited to around ±0.1 mr and the uncertainty in the polaroid index of refraction should be limited to around ±1 percent.

As the PAM equipment is further developed and installed, there may well be other potential error sources that will require analysis, e.g., parallax effects, prism misalignments, etc. To the extent that these are not calibrated or otherwise accounted for in the software, they will create attitude errors that may also have to be considered in configuring a system error budget.

n - Point Interpolators

n data points X_i and times of occurrence t_i ($i = 1, 2, .. n$) are specified. It is desired to pass a polynomial of order (n-1) through these points and then interpolate to find the value at some specified interpolation time t_I.

The required polynomial is given by

$$X(t) = \sum_{i=1}^{n} X_i \, A_i(t)$$

where

$$A_i(t) = \prod_{\substack{j=1 \\ (j \neq i)}}^{n} \frac{(t - t_j)}{(t_i - t_j)}$$

Check:

$$\chi(t_k) = \chi_k \qquad \text{for } k = 1, 2, \ldots\ldots n$$

For example, for n = 4

$$\chi(t) = \frac{(t - t_2)(t - t_3)(t - t_4)}{(t_1 - t_2)(t_1 - t_3)(t_1 - t_4)} \chi_1$$

$$+ \frac{(t - t_1)(t - t_3)(t - t_4)}{(t_2 - t_1)(t_2 - t_3)(t_2 - t_4)} \chi_2$$

$$+ \frac{(t - t_1)(t - t_2)(t - t_4)}{(t_3 - t_1)(t_3 - t_2)(t_3 - t_4)} \chi_3$$

$$+ \frac{(t - t_1)(t - t_2)(t - t_3)}{(t_4 - t_1)(t_4 - t_2)(t_4 - t_3)} \chi_4$$

The interpolated value $_I$ is then given by

$$\chi_I \equiv \chi(t_I) = \sum_{i=1, 2, \ldots}^{n} \chi_i A_i(t_I)$$

In the simulation n = 4 although the current PAM software shows n = 6. Some studies have also been performed using n = 8. Note that for PAM, t_I lies between $t_{(n/2)}$ and $t_{(n/2)+1}$ (n even). By using higher order

filters, the prism frequency can be lowered while maintaining the same overall accuracy. This requires more computer operations but if lowered prism speed is highly desired, this is a worthwhile trade.

Table 4-8 shows maximum errors as a function of n and the sampling frequency for a sine wave signal of 2 deg amplitude at a frequency of 1 Hz. The interpolation time corresponds to 90 deg phase, with the data points symmetrically disposed on either side of 90 deg. An n-point interpolator is a polynomial of order (n-1) and so passes perfectly a signal possessing only (n-1) (or less) non-zero derivatives. Interpolating a function with n or more derivatives such as a sine wave generally produces an error, with the maximum error occurring where the $n^{\underline{th}}$ derivative of the signal is a maximum. The $n^{\underline{th}}$ derivative of a sine wave (n = 2, 4 ...) is maximum at 90 deg (or 270 deg)*, hence interpolating at this point produces the maximum error for a given sampling rate. In Table 4-7, the n data points are equispaced around the 90 deg point. These are worst case results then in two respects, i.e., in the choice of 90 degs and the equispacing.

While a complete error budget has yet to be established, it seems reasonable to limit the interpolator error to 0.05-0.1 mr out of the total allowance of 0.25 mr. It is also desirable to keep the sampling rate (prism frequency) as low as possible, e.g., under 10 samples/sec. On this basis, n = 2 fails completely, n = 4 with f = 10 Hz is marginal, n = 6 with f = 7-8 Hz is satisfactory, as is n = 8 with f = 5-6 Hz.

*270 deg has been used in the simulation in choosing $t_{f\ell}$ = 0.75 secs with $w_v = 2\pi$ rad/sec.

TABLE 4-8. MAXIMUM ERROR IN MRADS FOR SEVERAL INTERPOLATORS AT VARIOUS SAMPLING RATES (2 DEG SINE WAVE AT 1 HZ)

Samples Per Sec	n=2	n=4	n=6	n=8
5		1.8	0.52	0.16
6			0.19	0.04
8			0.04	0
10	1.7	0.12	0.01	
12		0.06		
15	0.78	0.02		
20	0.44			

5.0 EQUIPMENT COMPLIANCE REPORT

OVERVIEW

This section documents the equipment compliance tests for the Exploratory Development model of the PAM. The tests were conducted on 23 November 1976 at the Hughes Aircraft Company facility in Culver City, California, under contract DAAB07-75-C-0810 with the USAECOM, CS & TA Laboratory. Mr. Frank J. Elmer is the ECOM Project Engineer for this program, and was present during the compliance tests.

The Exploratory PAM system consists of a ground tracking and computing equipment for the ground station and a cooperative airborne component for mounting on a Stationary Remotely Piloted Vehicle (SRPV). On board the SRPV will be a target sensor that outputs the angular orientation of a target with respect to the SRPV's coordinate system. The function of the PAM system is to monitor the position and attitude of the surveillance platform and compute the location of the target relative to a pre-selected ground coordinate system. Electro-optic techniques are used in the Hughes-developed PAM system to accomplish the system objectives.

The facility used for the PAM compliance test is shown in Figure 5-1. A survey using standard techniques was made of the test site to establish a series of known points, as indicated in the Figure, in a reference coordinate system. The ground station equipment was mounted in a trailer supported by jacks for stability, aligned such that the ground equipment's coordinate system coincides with the surveyed reference system.

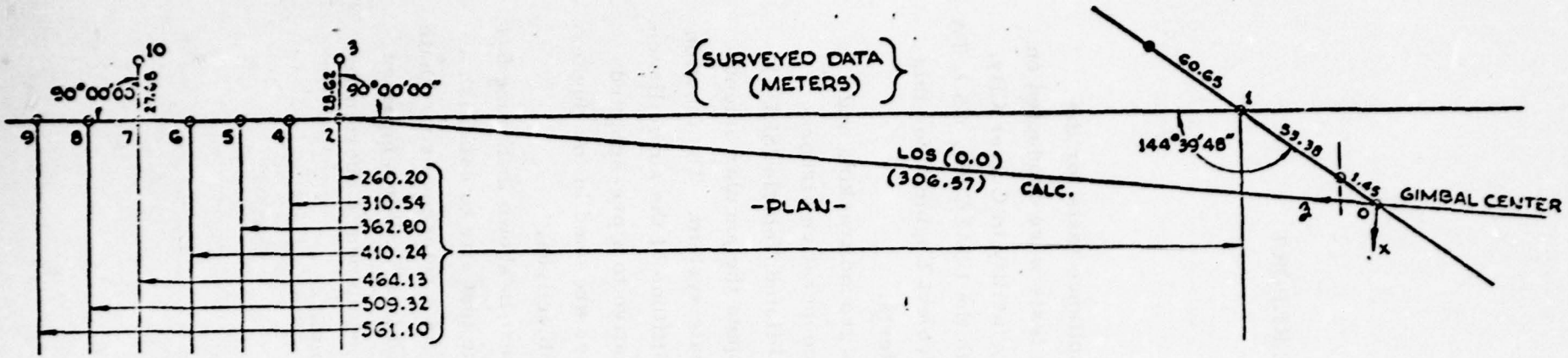

POSITION WITH RESPECT TO GIMBAL COORDINATE CENTER

POSITION	X	y	z
0	0	2.489	0
1	26.96	2.849	47.769
2	0	3.153	306.57
3	28.466	2.910	309.534
4	5.208	3.266	356.653
5			
6			
7			
8			
9			
10			

PAM TEST RANGE

Figure 5-1

POSITIONAL ACCURACY TEST

The following test was performed to demonstrate the ability of the PAM ground station to accurately locate the airborne component. An unpolarized corner cube was placed at known points and the ground station equipment used to measure the corner cube's location. The results of this test was that the positional measurement accuracy of the PAM is approximately 0.1 m well within the design specification of the technical guideline.

The tellurometer did not receive sufficient signal to allow the system to operate at 600 meters from a single polarized corner cube on the airborne component. This is felt to be an acceptable engineering tradeoff for the anticipated initial use of the PAM at altitude 450 m, near the lower limits of technical guidelines flight profile. At these lower ranges the principal difficulty lies in expanding the laser beam to fill the required effective aperture of the airborne component. A secondary difficulty at these lower altitudes is the near geometry situation which causes certain engineering approximations used in the original design to give less negligible errors (e.g., the two spinning porro prisms are assumed to be at the same point in the mathematical analysis when in fact they are about 10 cm apart).

TRACKING TEST

The following test was performed to demonstrate the ability of the PAM system to track the airborne component:

The airborne component cover was moved at a rate of approximately 10 meters per minute along the ground at a height of approximately one meter. The tracker followed well until it was confused by ground objects such as telephone poles in the background. In order to simulate better the intended use, the airborne component cover was moved to a height of approximately 3 meters off the ground and the test repeated with a sky background. In this case the tracker followed without confusion from clutter. (By installing a manual tracking gate, problems that arise in testing the PAM in ground clutter can be reduced.)

ATTITUDE TESTS

Static tests of the attitude measurement were performed. The airborne component was mounted on a test fixture to which a theodolite was attached. This test fixture was secured to a machinist's mount that has two orthogonal rotational degrees of freedom. The total airborne component was set up on a table at the surveyed points. The test fixture would be reoriented by adjusting the machinist table without changing the effective location of the airborne component. A small amount of cross talk existed between the two axes. See Figure 5-2 for the geometry of the airborne component.

PITCH-YAW TESTS

A second theodolite was temporarily set up in front of the airborne component. This theodolite was leveled and the airborne component reoriented until the spinning porro prisms swept the retroreflected reticle only horizontally and vertically respectively. The theodolite attached to the test fixture was then leveled and zero azimuth set in the direction of the ground station. In this way, the pitch/yaw axis of the airborne component corresponds to the two axis of the theodolite mounted on the airborne component.

Several convenient points were selected to take theodolite readings in order to determine changes in the orientation of the airborne component directly as data was taken. These readings also allow determination of the attitude matrix relating the theodolite and ground station coordinate systems via the "2 vector method." However, it was not feasible to compute this matrix while the static testing was in progress. (It was later discovered that the separation between the airborne component and theodolite would not allow the straightforward comparison of this matrix with that printed out by the PAM system. A method of easily computing the matrix and offset vector relating the theodolite and airborne component coordinate systems was subsequently devised by F. Elmer of ERADCOM.

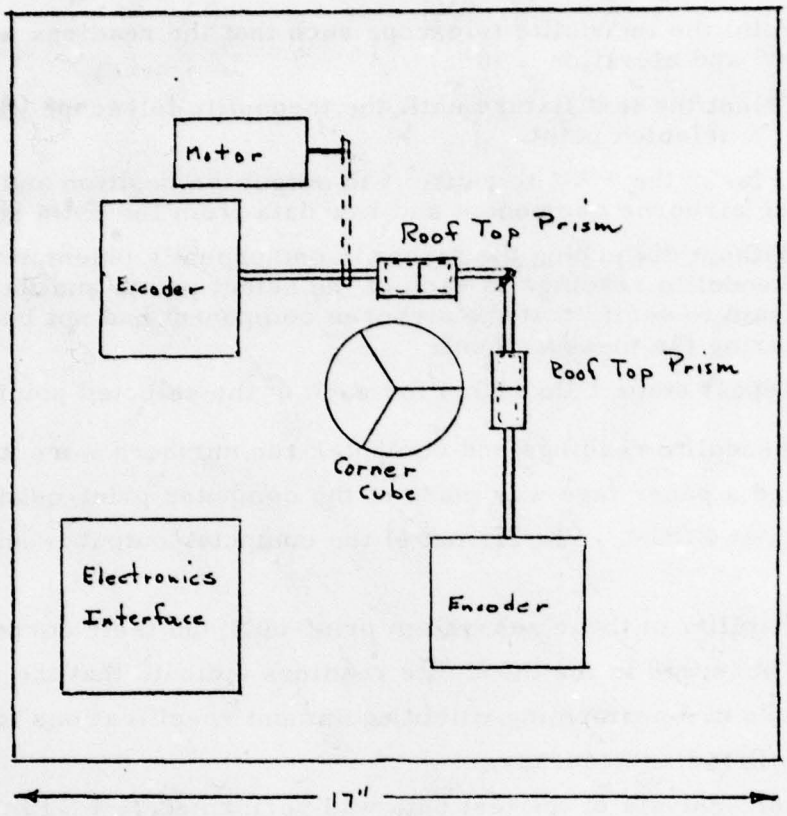

Figure 5-2. Airborne Component

The following procedure was used to conduct the static attitude tests:

1. Point the theodolite telescope such that the readings were azimuth =0° and elevation = 90°.
2. Orient the text fixture until the theodolite telescope was pointed at a selected point.
3. "Flash" the PAM to cause it to output the position and attitude of the airborne component and raw data from the PAM subsystems.
4. Without disturbing the airborne component's orientation, take theodolite readings to each of the select points and flash the PAM again to verify that the airborne component had not been disturbed during the measurement.
5. Repeat steps 1 through 4 for each of the selected points.

The theodolite readings and computer run numbers were recorded on data sheets and a paper tape was made of the computer print-out for later data reduction at ECOM. The format of the computer output is shown in Figure 5-3.

The stability of these subsystem print-outs and their correlation with changes observed in the theodolite readings indicate that the pitch and yaw subsystems are performing within equipment specifications to approximately 0.1 milliradian accuracy.

Further analysis of the test data was performed by F. Elmer at ECOM. The accuracy of the PAM attitude matrix was computed by assuming the airborne component and the theodolite to be at the same location, and then operating on the vector back to the ground station as read by the theodolite by the computed PAM matrix. This results in a vector which should be expressed in the ground station coordinate system and should be in the same direction as a vector from the location of the airborne component to the ground station as found in the ground station coordinate system from survey measurements. The angle between these two vectors is a measure of the accuracy of the PAM attitude matrix.

The accuracy of the computed PAM matrix for the orientations of the airborne component which differed from the original "aligned" or "zero reference" orientation by a few milliradians (less than 0.25 degree) were on the order of about 8 milliradian (0.5 degree). This degraded to about

TFLASH (IDENTIFICATION)

∠A	∠B	∠C	Range
∠D	∠E		

$$\begin{pmatrix} a_{11} & a_{12} & a_{13} \\ a_{21} & a_{22} & a_{23} \\ a_{31} & a_{32} & a_{33} \end{pmatrix}_{\text{Matrix}} \qquad \begin{pmatrix} X_0 \\ Y_0 \\ Z_0 \end{pmatrix}_{\text{Position}}$$

Computer Output Format

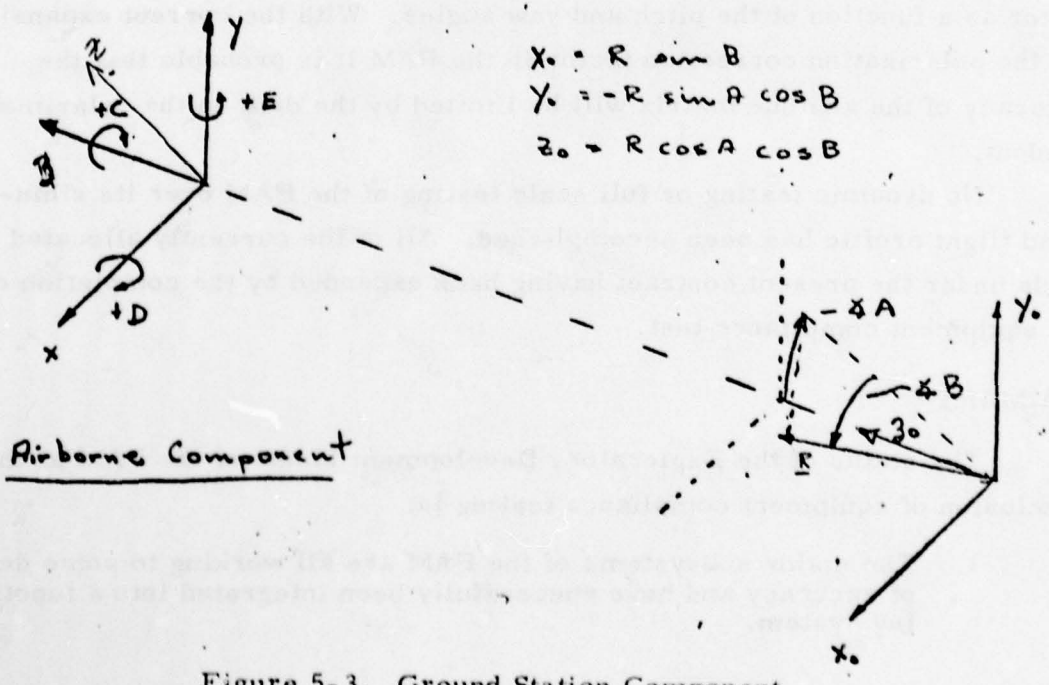

Airborne Component

Figure 5-3. Ground Station Component

200 milliradians (12 degrees) for an orientation of the airborne component which differed by about 6 degrees from the zero reference orientation. However, the matrix for the zero reference orientation was exactly correct.

Clearly this shows that an incorrect rather than an imprecise matrix has been generated. The generation of an imprecise matrix would have resulted in a nearly constant angular error instead of the trend of the errors observed. The errors discovered to have been inadvertently introduced by the misalignment of the theodolite and airborne component coordinate systems and the offset between the two could not exceed about 10 milliradians maximum.

The probable cause of the incorrect matrix being generated is the incorrect generation of the correction factor series expansion, in conjunction with the assumed coincidence and alignment of the theodolite and airborne component. This area requires further refinement of the test methods and the development of a method to derive the relationship and offset between the PAM airborne component and the theodolite from easily measurable data. Once this is done, it will be possible to derive what should have been the value of the roll input to the PAM algorithm and expand the correction factor as a function of the pitch and yaw angles. With the correct expansion for the polarization correction factor in the PAM it is probable that the accuracy of the attitude matrix will be limited by the drift in the polarimeter readout.

No dynamic testing or full scale testing of the PAM over its simulated flight profile has been accomplished. All of the currently allocated funds under the present contract having been expended by the completion of the equipment compliance test.

SUMMARY

The status of the Exploratory Development Model of the PAM at the conclusion of equipment compliance testing is:

1. The major subsystems of the PAM are all working to some degree of accuracy and have successfully been integrated into a functioning system.

2. The pitch, yaw, tracking, pointing, and computer subsystems have been demonstrated to the levels of performance required by the technical guidelines.

3. The retroreturn from a single polarized corner cube on the airborne component is insufficient for ranging at 600 meters, however performance below 450 meters is quite good and in view of the intended initial application of the PAM a reasonable engineering tradeoff in accordance with the technical guidelines.

4. Polarimeter subsystem performance is below that required in the following respects:

   a. The drift in the polarimeter readout under field conditions prohibits measurements to the accuracy required (drift is about 0.5 degree (8 mr)).

   b. The servo response is insufficient to follow a 1 Hz motion of the airborne component, and

   c. The current method used to rezero the polarimeter is not sufficiently repeatable to attain the desired measurement accuracy.

5. The packaging of the deliverable equipment is still in the brass-board configuration rather than to best commercial practice of a form that would allow subsequent testing of the PAM after delivery.

6. Visible radiation is used. There is no reason why the system cannot be extended for covert wavelength operation.

At the end of the equipment compliance testing a meeting was held between Mr. L. Hill (Hughes program manager), Mr. R. Kokron (contract specialist, HAC), Mr. F. Elmer (project engineer, ECOM), and Mr. H. Pardes team leader, ECOM). The status of the system was discussed and the work necessary to complete the original intent of the contract defined. A proposal for this effort was requested from Hughes.

ROLL TEST

The procedure for the roll test was to turn the theodolite 90^{o} so that its line of sight was perpendicular to the line of sight between the airborne component and the ground station. Roll angular changes were monitored with the theodolite while data was recorded. The polarimeter system did

not perform to system requirements. The following problem ares were noted:

1. Under static conditions the readout drifted over a range of approximately 0.5 degrees (8 mrads) instead of being stable to better than 0.1 mrads.
2. The method of attaching a reference polarized cube corner to the polarimeter did not result in acceptable repeatability for establishing a zero for the polarimeter.
3. The response time of the servo system was not sufficient to follow a 1 Hz motion of the airborne component.

Laboratory measurements at Hughes has shown that the theoretical correction factor, applied to the polarization measurement to account for non-normal incidence of the laser beam on the polaroid material, was not sufficiently accurate for use in the PAM application. Therefore, it was decided to take a series of measurements of the polarization measured for various values of pitch and yaw and use a series expansion to calculate the required correction factor. This was done and the resulting expansion incorporated in the computer program. (It was later discovered that the method used to reorient the airborne component did not necessarily preserve the "roll" about the line of sight as had been thought at the time.)

6.0 PAM SYSTEM MODIFICATIONS

The Position Attitude Monitor (PAM) system was removed from storage and the modification task assigned to Steve Sheldrake by John Nella, then Group Head, in the latter part of April 1977. The purpose of this section is to relate the modifications made on the PAM system, the reasons for these changes, and the current PAM status.

The PAM modification tasks which were undertaken were:

1. Rework of the polarimeter by Hughes Servo people under the direction of E. Maiuro
2. Complete system rewiring and recabling under C. Brown
3. Documentation and Test by J. Nella, S. Sheldrake, and G. Lundgren

The original group responsible for the PAM system were

1. L. Hill - Program Manager
2. J. Sneary - Electronics
3. J. Wagner - Computer and System Test
4. E. Maiuro - Gimbals and Airborne Component
5. B. Stokes - Mechanical Design
6. W. Buchmann - Optics and Polarimeter
7. J. Shrunk - TV and Tracker

These people were contacted, requesting information and documentation. The responses came in the form of logs, prints, and notes. Existing system documentation has been assimilated and presented.

The PAM device is comprised of three functional areas. These are the

1. Airborne Component
   a. Pitch and Yaw Spinning Prisms
   b. Roll Polarizer and Corner Cube
   c. Pitch and Yaw Encoders
   d. Three-axis Test Fixture
   e. Remote Flash, and Encoder Electronics
2. Gimbaled Pedestal
   a. Two-axis Motional Movement Driven by Stepper Motors and Encoders
   b. Gimbaled Component Table
      (1) TV Camera (Tracking)
      (2) Tellurometer (Range)
      (3) P&Y Receiver (Pitch and Yaw)
      (4) Polarimeter (Roll)
      (5) HeNe Illuminating Laser
      (6) Sighting Scope
3. Electronics and Data Processing Racks
   a. Rack 1
      (1) Polarimeter Electronics
      (2) Pitch and Yaw Electronics
      (3) System DC Power Supplies
   b. Rack 2
      (1) Gimbal Azimuth Driver
      (2) Gimbal Elevation Driver
      (3) Polarimeter 400 Hz Power Supply
   c. Rack 3
      (1) TV Monitor Display and Gimbal-Tracker Controls
      (2) System Power Control and HeNe Source Supply
      (3) Computer Unit
      (4) Disc Memory Unit
   d. Data Input-Output Teletype

Optical Mounting of the P&Y RCVR, POL, and LASER

The geometrical locations of the helium neon illuminating laser (HeNe), the pitch and yaw receiver (P&Y RCVR), and the polarimeter (POL) were relocated. Several deficiencies in the previous design were thus corrected.

The HeNe beam previously was folded by two prisms and projected from in front of the P&Y RCVR and POL. Multiple surface reflections, and scattering caused erroneous detected energy, both operationally and when a polarization reference fixture put this output directly into the POL. Two first surface mirrors, a beam steering fixture, and bringing the beam through a lens holding aperture from behind the P&Y RCVR and POL apertures, solved these problems. The ability to insert lenses both positive and negative facilitates laboratory testing and field optimization (beam size control).

In addition, the HeNe beam exists from the geometrical centerline of the P&Y RCVR and POL input apertures. Both of these apertures were brought as close together as physically possible. The retroflectors return beams, return at twice the physical size of their input apertures. These returns are centered on the laser output. Previously one return from either pitch or yaw just barely entered the P&Y RCVR. Any scintillation resulted in missing pulses. Now, due to relocation half of the energy from these returns is detected.

Polarization Reference Fixture

A polarization reference fixture was constructed to provide a means to set the polarimeter zero repeatably. This is required since any time the reset is depressed, the polarimeter reading sets to zero. The airborne component has a vertical polarization reference axis. The HeNe laser beam is folded by two first surface mirrors and passes through a rotatable piece of polarizing material. The fixture is indexed and can be put on and taken off. The rotatable piece of polarizing film now is set for a vertical reference polarization.

Procedure for field testing will be to attach fixture, depress POL reset button zeroing the display, and not resetting the zero unless the fixture is attached.

Rewiring - Cabling - Relocation of Components

One of the major purposes for the PAM system modification was the complete rewiring of the system. This item also has accounted for the most delay and expense which beset the modification task.

As received, the system was a myriad of assorted cables, test boxes, connectors, power supplies and fixtures. The PAM system rewiring was given to a designer under the direction of K. Brown. While delays resulted due to the design incorporating of industry wide out-of-stock connectors, the end result has good engineering. Setup will be quick and straightforward.

All gimbal components attach to either a gimbal pedestal mounted panel or the TV tracker electronics box. From the pedestal a single umbilical connects the pedestal with the PAM electronics. This umbilical goes to the rear of the computer housing rack, whence it is distributed to the appropriate racks and electronic packages. Some items were relocated or discarded to achieve the simplest distribution arrangement. AC power, as well, is controlled by a central power switch and distributed to the three racks and teletype.

Cable diagrams and a master wiring diagram are provided.

System Flash-Remote-Local-Motional Flash

The original flash pushbutton to initiate the computer program has been expanded. The computer can be flashed locally, by a manual momentary switch, remotely at the airborne component by another manual switch, or by a motional sensor (LED-Photodiode) on the yaw rotational test fixture table.

The data cable contains three twisted wire pairs. The first two contain pitch and yaw encoder data. The remaining twisted pair was used to

transmit the signal from the two remote sensors to the computer front panel. Here a switch selects the mode, remote or local, and this selected signal flashes the program.

For local operation, the switch is set to local and pushbutton depressed. However, for remote operation the following procedure applies.

1. Computer panel select switch to remote
2. Enable switch on airborne component electronics box to enable (red light indication)
3. Manual flash by pushbutton
4. Or, motional flash by LED-Photodiode when the open slot allows LED energy to reach photodiode.

The enable switch is to prevent false remote triggering (mainly from motional sensor) and motional triggering in only one direction. This was required since all flashes accidental or not are processed and the data is entered on the data storage disc.

On the front panel of the computer rack a two-position switch selects the flash mode either local or remote. In the local mode, a pushbutton switch is depressed to simulate a flash. For remote flash and automatic computer flash during motional tests, the switch on the front panel is set to remote.

At the airborne component test fixture, a similar pushbutton will flash the computer when

1. Panel switch set to remote
2. Remote box switch set in enable
3. The motional flash sensor is optically blocked

For motional tests the LED photodiode sensor is set to a blocked position, the box switch enabled, and the rotary table scanned to the open slot position. For repeatable results, the sensor should be disabled, returned to the original starting point, enabled, and the scan done again. This one direction scan should eliminate mechanical motion slop in the rotary table motion.

Remounting of DC Power Supplies

Previously, the TV ±24 supplies were located within the azimuth and elevation gimbal driver boxes. These were incorporated into the DC power box. The meter switching function was expanded to allow monitoring of these additional supplies.

The DC power supply box now houses

1.	+20 VDC	Pitch and Yaw RCVR
2.	-12 VDC	Tellurometer
3.	±24 VDC	TV and Tracker
4.	+5 VDC	All logic circuits

Remounting of Laser Supply

The laser supply was mounted in a power control panel in the computer rack. This allows front panel control of the laser power, insures that HV cable cannot be disconnected with supply on, and provided space to print safety warnings and lights for laser beam warning.

System Power Control

A master power control switch controls a power contactor. AC power to the three equipment racks and teletype is thus controlled by a single switch.

Pitch and Yaw RCVR

The pitch and yaw RCVR was relocated as discussed previously. This required that the long tubular structure be shortened. This was accomplished by folding the electronics package.

As part of the testing it was found that the HeNe interference filter on the Meret detector was defective. Its transmission was less than 6 percent when it should have been approximately 60 percent. A color glass filter was substituted with 90 percent trandmission. The combination of the orange-red cutoff of the filter and the detector near IR response results in an effective 100 Å bandpass.

The electronics were also extensively modified with addition of 1 μf filter capacitors in parallel to those existing and at the detector bias pin to reduce noise and increase fast pulse response. The electronics used a highpass filter (capacitive coupling) with caused differentiation and multiple pulsing for the slower lab test and short range pulsewidths. This value was increased to allow this essential testing ability.

A MA 94 preamp was destroyed during soldering and has since been replaced.

During field testing it was found that most data could only be taken by late afternoon. This forced the RCVR to always look towards the horizon and into the afternoon and setting sun. This causes saturation of the first amp (DC coupled) and no P&Y yaw signals. A second 0.6328 interference filter surfaced and was incorporated. This solved both the sunlight saturation provided 60 percent transmission.

Polarimeter

The polarimeter was reworked by Hughes Servo people. However, several technical oversights by these people and their liaison required that the polarimeter be further reworked and modified. In essence, the servo people dealt strictly with the servo driver, the previous PAM personnel with only the motor and 400 Hz reference, both without regard to the polarimeter signal processing.

The following changes were required. A loss of signal cutout relay, to disable the servo when the HeNe return is temporarily blocked, was erroneously put in a servo motor phase winding. A motor control winding was provided and already had a mechanical interlock switch disable. As it was hooked up, cutout was erratic, required constant adjustments, and caused wild oscillations of the servo response for fluctuating laser signals. The relay switch was put in series with the interlock switch in the proper control winding. Circuitry sensing the voltage applied to the PMT is monitored to open the control winding. A buffer amp, followed by a comparator, drives a relay driver transistor. A front panel potentiometer supplies the reference voltage for the comparator. Thus, the level of cutout is easily

adjustable. A LED light indicator provides a usual indication of when the servo motor is disabled. A normal pot setting is 9.0.

The phase locked loop drive frequency (servo ref) and the motor were changed by previous personnel. The PLL also functions as a clock driver for a very narrow band digital, synchronous, filter to sense the fundamental (400 Hz) and second harmonic (800 Hz) frequencies. The processing amplification stages and center frequencies were not charged. The result was a badly distorted, attenuated, and phase shifted error signal. The servo people also ignored this and subsequently added large gain, and phase correcting circuitry, to try and fix the servo performance.

The polarimeter electronics were modified by the following steps

1. All amplifier filters were scaled to account for the 60 to 400 Hz frequency change.
2. The center frequencies of the digital filters were moved to 400 and 800 Hz from 60 and 120 Hz, respectively.

Due to difficulties in removal of the servo added stages, these were left. The polarimeter now functions very stably with damping and gain adjustments at minimums, after a 1 hour warmup.

One difficulty not addressed is a noise induced switch of the 0.0 digit to 0.1 without accompanying servo motor motion. Since, this and slow numerical drifts, do not occur after sufficient warmup it did not warrant the time and money to diagnose and correct the situation.

Electronic Test Monitoring

BNC test monitoring outputs were added to allow laboratory testing and rapid malfunction location ability. The following describes these points.

The front panel on the polarimeter and pitch and yaw electronics rack contains BNC output connectors to monitor

1. Fundamental (400 Hz) Digital Filter Output - Normal
2. P&Y RCVR Output - Differential
3. Pitch Encoder Output - Differential
4. Yaw Encoder Output - Differential

The fundamental digital filter output provides a valuable signal to evaluate the polarimeter operation. At a null position of the polarizer the signal is a digital (step) representation of the 800 Hz second harmonic. At positions off null and when servo is driving towards a null, it will be a distorted wave-shape containing 400 and 800 Hz components. Its existence, of course, indicates a received corner cube return.

The pitch and yaw RCVR output will show two negative pulses indicating returns from the pitch and yaw signals, as received by the P&Y RCVR. Within a 10 Hz period (100 msec) two such pulses indicates both pitch and yaw returns.

The other two monitors are the raw encoder signals (90 kHz) from pitch and yaw after transversing the data transmission line (300-600 meters).

Airborne Component

The airborne component underwent extensive modifications to facilitate easier operation at the field test, and to correct areas of concern.

The prisms, and corner cube were relocated, in addition to changing the method of drive. The corner cube was mounted in the center of the optics table. The prisms were mounted as close as possible to the corner cube. The roof line of each prism was made to align to the x and y local axes of the optics table. New shafts replaced bent ones, direct motor drive, and anti-backlash gears were used to couple the two spinning prisms. Previously, the encoder outputs indicated serious FMing of their outputs due to rotational fluctuations, and missing signal gaps. The modifications have reduced the FMing to a reasonable level, and continuous signals are now observed. Metal parts were black anodized, and in conjunction with a white dust cover with appropriate open aperature, form a easily trackable contrast target for the TV tracker.

The previous breadboard electronics were redone and housed in a switchable box with self-contained 5 VDC supply. Monitoring parts of the raw encoder outputs (signal and sync) and the data signal (sync derived missing pulse data train) are provided. The only power required is 120 VAC. A battery and inverter will be used.

Field Test Fixture

The previous test fixture for three axis motion has been replaced. Originally a single machinist's table with two axis tilt and single axis rotation was used. Thus motions were not independent. Roll motion was experienced for tilt motions. In addition, the actual mounting of the optics table required a long lever arm. This created motions of the measuring theodolite that completely masked the results in real time. A correction matrix would allow compensation of this static error however.

Instead, two rotation tables, one with tilt, now provide 3 axis independent motions. The airborne component is mounted to a small rotary table with the rotation providing roll motion. Tilt motion of the same table about the horizontal, provides pitch changes. Lastly, a large rotary table and offsetting fixture provide yaw motion.

Unfortunately, the theodolite axes and the airborne component axes must be physically displaced. Correction matrices will need to be generated to account for these offsets between the measured and actual data.

Gimbal Pedestal

The gimbal pedestal was modified to fix detected defects.

The upper body was rotated in relation to the tripod legs to provide support along the best directions. The TV tracker box was relocated forward and up to move it out of an operator's knee area.

The gimbal providing horizontal rotation was found to have excessive, and a woodruff key that was too small. Bumping easily rotated this gimbal (clutch play), and half inch free travel motion (gears and Keyway) would have caused errors in this axis. These problems were remedied.

No modifications were made to the vertical axis rotation gimbal.

Present Operational Instructions

The following will present a somewhat arbitrary initialization procedure to bring the PAM system to operation. Exact order is not necessary, but following that listed will assure all components are functional.

1. Turn on the main system power switch located on the left hand side, second panel from top of the computer rack. Power will

be supplied to the teletype, computer rack, pitch, yaw and roll rack, and tracker driver rack. REMEMBER THIS SHOULD BE THE FIRST AND LAST STEP (DURING SHUTDOWN) TO PROTECT DISCS FROM ERASURE.

2. Turn on the computer using the keyed switch. Press halt.

3. Turn on disc driver. Left Protect/Enable switch to enable.

4. Turn on DC power supplies. Switch located on bottom panel of Pitch, Yaw, roll electronics rack. Using meter monitor switch, monitor voltages from each supply. Disregard exact voltages, use only for approximate go/no go check.

5. Turn on television display. Pull out on Brightness/Power Knob. Allow time for warmup and adjust brightness and contrast for best display.

6. Turn on 400 Hz 120 VAC supply located on bottom of tracker driver rack. Two on switches must be moved to the up position. Turn on line power switch in center. Allow short time for warmup. Using volts/adjust knob adjust voltage to 120 VAC. Turn output switch on.

7. Turn Loss of Signal potentiometer on polarimeter panel to a setting of 5.0 or less. This will disable servo loop during warmup. Red indicator light should light.

8. Depress polarimeter Power switch. Polarimeter will come on and LED display will light up. Allow at least 1 hour warmup before attempting measurements.

9. Turn Azimuth Driver power switch to on. The following switch settings are for either remote (small control box which plugs into TV electronics box on pedestal) or local (controls on TV display panel) operation. For operation from the tracker driver panels a different procedure is required.

   a. CCW/CW switch to its center position

   b. OSC switch to its up position

   c. SPEED switch to its down position

   d. SPEED ADJ fully counter clockwise

10. Turn Elevation Driver power switch to on. As above set,

   a. CCW/CW switch to its center position

   b. OSC switch to its up position

   c. SPEED switch to its down position

   d. SPEED ADJ fully counter clockwise

11. For operation from the tracker driver boxes both azimuth and elevation switch positions are

    a. CCW/CW switch to desired direction

    b. OSC switch to its up position

    c. SPEED switch controls application of motion. Switch up to slew

    d. SPEED ADJ set to desired slewing speed

12. The monitoring outputs should be hooked to a suitable dual trace scope.

    a. Polarimeter Digital Filter Monitor

Vertical	200 mv/div
Horizontal	1 ms/div

    b. Pitch and Yaw RCVR Monitor. Must be monitored using both BNC outputs into a differential plug-in.

Vertical	5 volt/div
Horizontal	20 ms/div

    c. When desired the Pitch and Yaw encoder outputs can be monitored to assure these signals are being received over the data transmission line. Both are mounted differentially.

Vertical	2 volt/div
Horizontal	10 μs/div (90 kHz data)

13. Turn on teletype using off/on switch on teletype.

14. Turn on tellurometer using switch on the gimbal mounted unit. Turn setting fully ccw without turning off.

15. The PAM system now is powered up.

For normal operation (ONCE DISCS ARE REMOVED) only the main power switch need be turned off and on.

7.0 PAM PRE-ACCEPTANCE TEST REPORT

Test Goals

The goals of the PAM field testing are 1) to demonstrate the basic feasibility of the approach selected to implement the various subsystems, 2) to evaluate the individual performance of these subsystems, 3) to demonstrate the positional accuracy of the PAM in locating the airborne component relative to the ground station, 4) to demonstrate the accuracy with which the PAM system can determine the attitude of the airborne component and that of the simulated target sensor rigidly attached to it, and 5) to demonstrate the basic concept of the airborne Passive Artillery Locating System (PALS-A) by locating a cooperative target in the ground station coordinate system from a target sighting made by the sensor rigidly attached to the PAM airborne component.

Test Set-up

The ground station and associated equipment was set up in the back of a jacked up truck as shown in Figure 12. The stability of this arrangement was checked using a master level and shown to be on the better than 0.05 mrad worst case. The actual stability during testing was approximately 0.001 mrad. This was traced to flexure of the wooden truck bed rather than any problem associated with the truck body as supported by the jacks. The airborne component/theodolite mounted on its modified machinist's table was placed on a leveled heavy wooden office table. The stability of this arrangement was not specifically measured, but observations of the bubble level on the theodolite indicated negligible motion during setup and initial testing.

The positioning stakes were set up as shown in Figure 7-1 to form a cross pattern at the 300 meter range. These stakes were set out by first leveling the ground station and then walking out to 300 meters along the Z axis of the ground station using the ground station telescope line of sight as a guide. An unpolarized corner cube was used to allow the PAM tellurometer to measure the range to each of the stakes. The stake at point M was then driven in. Another stake was driven in about 20 meters behind M at N. Another stake was driven in about 20 meters in front of M at L. This established L, M, N and the ground station to be colinear in azimuth.

Two additional stakes were driven in approximately perpendicular to this azimuth on either side of M at J and K. A theodolite was then set up over the stake at M and leveled. An aiming stake was prepared by placing bands of tape around a long thin board. This aiming stake was then placed vertically on top of each of the stakes L, J, N, and K and theodolite readings taken to each of the bands on the aiming stake. The known distance between each of the bands on the aiming stake and the angles read by the theodolite allows the range to the aiming stake to be computed and the location of the top of the stakes L, J, N, and K to be computed relative to the top of stake M. The locations calculated by this technique were compared to the results of a survey using the PAM ground station to sight on an unpolarized corner cube held on top of the respective stakes. The locations of 3 of the 4 stakes matched within 0.2 meter, while the other showed a significant discrepancy. This was subsequently discovered to be due to a procedural error in reading the theodolite. Results of the equipment compliance test in November 1976 conclusively demonstrated the survey accuracy of the PAM ground station to be within 0.1 meter consistently. Thus the decision was made to use the results obtained by the PAM survey as the "correct" location of the respective stakes.

Two sighting stakes were driven about 40 meters in front of the ground station and 10 meters to either side of the line to the positioning stake M from the ground station. The tops of these two stakes were designated P2 and P3 respectively. The ground station center of gimbal was designated as P1.

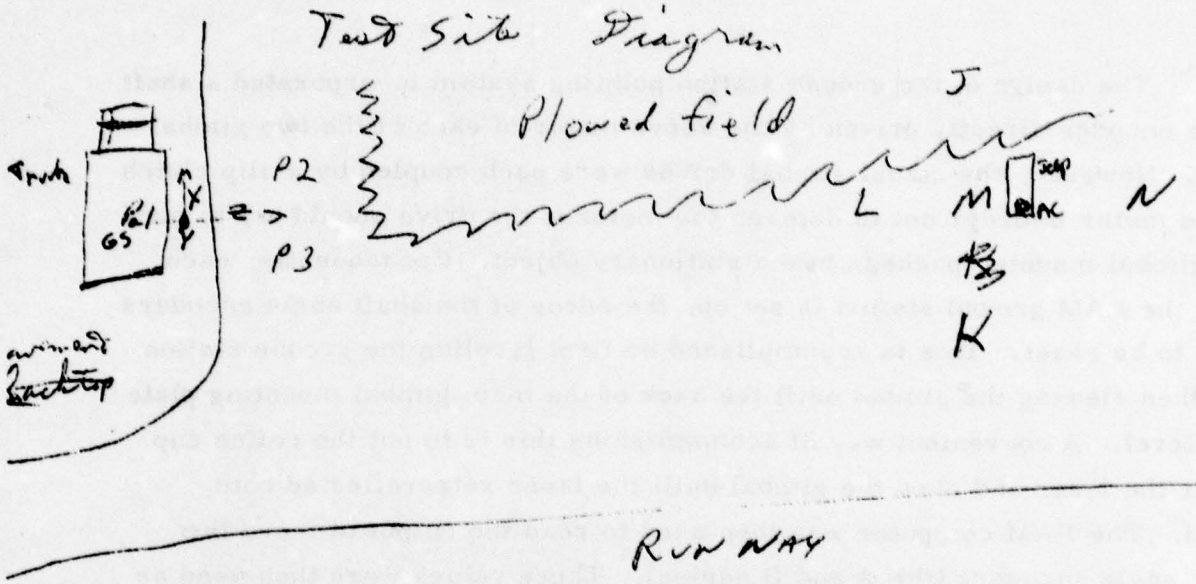

Point	Location according to			PAM survey	
N	.42,	-2.08,	319.49	.28, -2.19,	317.49
M	.39,	-2.32,	299.89	.26, -2.30,	299.89
L	.37,	-2.17,	280.89	.19, -2.12,	280.89
J	19.75,	-2.14,	299.74	19.57, -2.02,	299.75
K	-18.49,	-1.96,	299.82	-18.54, -2.02,	299.82
~~P2~~					
~~P3~~					
P2	8.55,	-1.97,	41.79	W track	
	8.69,	-1.82,	41.77	Laser track	
P3	-9.65,	-1.90,	40.94	W track	
	-9.55,	-1.78,	40.96	Laser track	

4 Feb

Airborne Component location during test:
-1.85, -1.59, 303.19

Airborne Component to theodolite separation:
0, .40, .18

Figure 7-1.

The design of the ground station pointing system incorporated a shaft angle encoder directly driven by the servo motor in each of the two gimbal axes. However, the actual gimbal drives were each coupled by a slip clutch to the motor in order not to damage the motor if the drive should try to turn the gimbal mounted package into a stationary object. Consequently, each time the PAM ground station is set up, the zeros of the shaft angle encoders have to be reset. This is accomplished by first leveling the ground station and then slewing the gimbal until the back of the main gimbal mounting plate was level. A convenient way of accomplishing this is to put the coffee cup under the laser and slew the gimbal until the laser retroreflected onto itself. The PAM computer was then used to read the output of these two shaft angle encoders (the A and B angles). These values were then used as offsets subtracted from the measured values to obtain the values corresponding to the mathematical definition of the A and B angles.

The offsets for the porro prism shaft angle encoders which measure the D and E angles also use offsets which must be empirically determined. The procedure for determining these offsets is as follows:

1. Set up the airborne component/theodolite at the nominal 300 meter test position.
2. Mount the flat first surface mirror on the front of the polarized corner cube.
3. Point the theodolite at its nominal setting of 0 azimuth, 90 degrees elevation.
4. Orient the airborne component/theodolite until the ground station appears in the crosshairs.
5. The reflection from the mirror should be in the vicinity of the ground station. Have the ground station operator find the reflection and guide the airborne component/theodolite operator in reorienting the unit until the reflection is recentered on the laser.
6. Flash the PAM to read the D and E angles.
7. Take the most often occurring value in the 6 readings recorded for each angle and use that value as the offset for the respective angles.

Initially the television camera was used to see the mirror reflection, but resulted in a burned spot on the camera tube which made tracking

impossible until the television camera tube was replaced. The attempted use of the bright spot from the polarized corner cube in normal operation for tracking showed that when locked on, this worked fine. However, if the reflection was not centered, the movement of the tracker tended to reduce the intensity of the reflection rather than increasing it. This resulted in the tracker moving further off target until track was completely lost. Therefore, it was recommended that the future versions of the PAM make the television blind to the laser used to illuminate the airborne component. Contrast tracking of the airborne component was shown to be quite good, however, the tracking electronics used appears to get confused by objects in the background. This can easily be fixed in future versions by installing a manual rather than an automatic gate in the tracker. The tracking ability of the PAM against a sky background was demonstrated conclusively during the equipment compliance testing in November 1976 by holding the cover of the airborne component on a stick to get a view with a sky background. Even more dramatically, during the pre-acceptance testing it was demonstrated that the PAM could track seagulls walking on the grass near the end of the runway alongside the test site.

The most problems were encountered with the polarimeter subsystem. The polarimeter was a commercial instrument designed originally to measure the concentration of sugar in solutions via the amount of rotation induced in polarized light shining through the sample. For this application, an incremental shaft angle encoder is ideal. However, for the PAM, an absolute encoder should be used. A "calibration fixture" was fabricated to reflect the laser beam through a polarizing filter and into the polarimeter. This did indeed provide a very convenient way of initializing the shaft angle encoder output counter to zero when the system is first turned on and had locked into the polarization of the reflected beam. The problem was that it was impossible to replace the calibration fixture on the polarimeter exactly the same way each time within the accuracy of the instrument. It was shown that the polarimeter had no trouble returning to the same count each time the beam was interrupted and then allowed to resume. Therefore, it was decided that the way to put a "zero" on the polarimeter was to place marks on the gear train driving the analyzer from the servo motor. The polarimeter

could then be turned on and driven to near the "zero" setting by the "calibration fixture." The servo was then disabled and the gear train turned to the "zero" position by hand. The reset was then pressed to zero the shaft angle encoder output counter.

The major problem created by this was that there appears to be no simple way of setting the zero of the polarimeter to correspond with the mathematical definition of the polarization angle which the polarimeter is designed to measure. During the testing, it was determined that by using the theodolite's calculated attitude via the two vector method to get the attitude of the airborne component the "actual" polarization angle that should have been measured could be calculated. The difference between the "actual" and measured values should be some constant offset term plus the "correction factor" described above which is a function of the D and E angles. This could be later analyzed to provide the appropriate offset and coefficients of the correction factor power series to be used with the PAM during further testing.

By the time these and other minor problems were corrected, heavy rains in the area resulted in the test area being lightly flooded. It became impossible to set up the airborne component near point M using the table as had been done previously. To overcome this problem, a jeep was borrowed and the PAM airborne component installed on it. The pre-acceptance test was performed 11 February 1978.

The leveling of the ground station was checked. The appropriate A, B, D, and E angle offsets were entered into the PAM program. The polarimeter was zeroed as described above. Consistent range readings were being obtained by the tellurometer. The pointing of the ground station at the airborne component was maximized for best pitch/yaw returns and the television tracking system was disabled.

The weather was generally sunny with a slight wind and a few dark clouds. The humidity was fairly high and scintillation was noticed when looking at the airborne component from the ground station. As the test progressed, it became increasingly cloudy with the polarimeter drift apparently improving with the decrease in apparent scintillation. At the

conclusion of the test, the pointing stakes P2 and P3 were resurveyed using the PAM. Slightly differing readings were obtained when the television camera was used to lock on to P2 and P3 than when the laser beam was centered on P2 and P3. These differences are explained by the separation between the television and laser subsystems on the gimbal mounted sensor package.

For the static test at each of the 29 selected orientations of the airborne component/theodolite the following procedure was used:

1. The theodolite operator sets the telescope of the theodolite to point in the direction specified by azimuth and elevation angles radioed by the ground station operator.
2. The airborne component/theodolite assembly is reoriented until the telescope crosshairs point at the center of the ground station gimbal.
3. The theodolite operator then radios the exact theodolite readings to the ground station operator.
4. The ground station operator flashes the PAM, records the readings and the most significant digits of the time of flash printed out by the PAM computer as the run number.
5. The theodolite operator then takes a theodolite reading to P2, being very careful not to disturb the orientation of the airborne component.
6. The theodolite operator then radios the readings to the ground station operator.
7. The ground station operator then repeats step 4 above.
8. The theodolite operator then repeats steps 5 and 6 above sighting on P3.
9. The ground station operator repeats step 4 above, then the above procedure is repeated for the next orientation.

One additional static test was performed with the theodolite being level. Afterward, simple theodolite readings were taken to the positioning stakes L, M, J, and K.

At the conclusion of the static testing, the shutter and optical switch are attached to the machinist's table and tested. The machinist's table is cranked dead slow until the orientation "selected" by the shutter/optical switch is reached. The same procedure for taking and recording theodolite

readings to the ground station (P1), P2, and P3 is followed as for a static test (steps 3 thru 10 above). The machinist's table was then cranked several degrees to one side. The PAM was readied and the machinist's table cranked smoothly several degrees past the "selected" position which automatically flashed the PAM. The first four runs made in this fashion were done with moderately fast cranking. The next four were done with slow cranking, and the next two were done dead slow. The approach to the selected position was made from alternating sides using this approach.

Next, the jeep was moved slightly after the tracking had been enabled. The PAM tracked the airborne component mounted on the jeep. Another set of theodolite readings was taken from this new position and orientation. This procedure was repeated a total of 5 times before a disc malfunction forced termination of the testing.

Immediate Conclusions from the Pre-Acceptance Testing

Immediately following the conclusion of the pre-acceptance testing, a photographic session was held to document the test set up and conditions before the equipment was removed from the test site. Arrangements were made to ship the PAM to Ft. Monmouth for final acceptance testing as specified in the contract. Due to the many problem areas encountered during the test, and the loss of the test data stored on disk, it was decided to wait until the equipment reached Ft. Monmouth before attempting any extensive data reduction. However, a preliminary partial analysis of the data was performed during the test itself to check for obvious malfunctions.

Such a malfunction was noted in the D and E angles. At the beginning of the work with the PAM, they showed very good consistency (on the order of 0.1 to 0.2 milliradians). However, shortly after starting the pre-acceptance test, the D and E angles both suddenly jumped from a few milliradians to nearly 1.5 radians. As this data appeared to be roughly consistent, it was decided to continue with the test and account for the apparent sudden change in offset later. The variation in the D and E angles for some orientations still appeared to be around 0.2 milliradians, therefore it was erroneously concluded that the pitch and yaw circuits were working correctly.

Another obvious malfunction was the drift in the polarimeter readings during the test. This drift was observed to be on the order of 5 milliradians during the worst period of scintillation to as little as 0.1 mrad during the quieter periods. The difficulty in resetting the zero on the polarimeter using the "calibration fixture" (repeatable to no better than 1.6 mrad) was also a serious deficiency in the testing.

While actually using the equipment, the effects of separation between the various optical components became quite noticeable. While this is a subtle design flaw, it does explain many of the problems with

On the positive side, the computer disc, teletype, tellurometer, television camera and tracking electronics, the ground station pointing system, tether cable, and theodolite worked quite well. The PAM did exhibit a positional measurement accuracy of better than 0.1 meter.

The operation of all of the PAM subsystems within the required accuracies was demonstrated at some point during the test which establishes the basic feasibility of the PAM approach. The subsequent analysis of the test data does establish the basic validity of the novel test techniques based on the two vector method which were developed for the PAM. These techniques, by themselves, are a significant advancement in the state of the art.

Considering that the PAM is in its exploratory development phase, the pre-acceptance testing of the PAM can be considered successful on the basis of establishing system feasibility, identifying refinements necessary to improve PAM performance to the level required for a practical system, and validating the use of the novel techniques developed for the testing of remote attitude measurement systems.

Pre-Acceptance Test Data

The disc malfunction at the end of the pre-acceptance test left only the PAM program printout and filled in data sheets for test analysis. The appropriate values were transcribed to summary working data sheets and entered to the various computer programs as described above in order to

calculate the attitude of the theodolite and thence the "correct" values of the C, D, and E angles from the simulation program PATDS. The two sets of "surveyed locations" for the stakes N, M, L, J, K were made several hours apart on 4 February 1978. A quick analysis of this data shows that the PAM repeatably surveys positions to within 0.1 meter. Comparison of this capability with the results of the equipment compliance test which used independently surveyed points, establishes the accuracy of the PAM survey results.

The closer range of the points P2 and P3 illustrate the problem introduced because the television camera and the laser are not at the center of the gimbal mounted sensor package. Readings to these two points were made within minutes of each other, one tracking the point with the television, and the other by slewing the laser beam to illuminate the same spot. The locations of P2 and P3 as determined by the laser were used in the reduction of all data.

The location of the airborne component as surveyed by the PAM remained constant during the test. The mounting arrangement allowed the effective center of the airborne component to move by no more than 3 centimeters and the effective center of the theodolite to move by no more than 4 centimeters from their nominal positions. The separation between the theodolite and the airborne component was measured using the center of the polarizing filter on the corner cube as the effective center of the airborne component and the center of the telescope as the effective center of the theodolite.

All reduced data are listed at the end of the section. The first 29 static orientations were selected to give a good sampling of the possible orientations of the airborne component permitted under the limited flight profile specified for the RPB in the technical guidelines.

Such a sampling would allow a calculation of the coefficients of the power series in D and E for the correction factor applied to the polarimeter. As mentioned above, the drift in the polarimeter and the unexplained sudden offset of the D and E angles make it impractical to do this calculation.

The 30th test was done with the AC/theodolite oriented such that the theodolite was level. The 31st test was done to define the static "reference" orientation of the AC/theodolite which was used for the dynamic test. The values of C, D, and E obtained were averaged over the 2 static and 10 dynamic runs to obtain the mean values shown for this test.

The format of all 31 orientations listed in Table 10 is the same. The "mean" value of the C, D, and E angles were computed after discarding any obviously erroneous data. This occurred on only a few runs and for the most part, all three measured values were used. The "+ or -" line shows the variation in the respective C, D, and E angle measurements. When all three readings were used, the standard deviation of the data was taken. When only two readings were used, one half of the difference between them was shown.

The theodolite readings shown were used pairwise to compute the attitude of the theodolite using the 2 vector method. The principal axis and angle of rotation obtained was used in conjunction with the position of the airborne component, separation between the airborne component and theodolite, assumed alignment of the airborne component with the theodolite coordinate systems, and the locations of P2 and P3 to simulate PAM behavior in the PATDS program. This program gives what a perfect PAM would have read if the airborne component were actually at the given location and in the given orientation. The values of C, D, and E thus calculated are shown in the line titled PATDS. The difference between the PADTS "correct" values and the measured mean values is given in the line below. Ideally, this entry would show only the measurement "noise" in the system and would thus give an indication of the accuracy of the respective subsystems. However, the unexplained, apparently constant offset in the D and E angles masks this. The offset in the polarimeter output, C, is due to the use of a mechanical zero as described above. This was set at a convenient location with the intention of correcting for the offset induced during the data reduction process in the automated data reduction system. Thus the best measure available of the individual subsystem stability and therefore "accuracy" if the proper offset had been used is the "+ or -" value.

Another feature of the PATDS program is the calculation of what the theodolite readings would have been if the theodolite were actually offset and oriented as described from the airborne component. These simulated readings are shown in the two columns labeled PATDS AZ and EL. The angular difference between the vectors represented by the actual and simulated theodolite readings is shown in the column labeled angular error. This is actually a measure of the accuracy of the principal axis and angle calculated for the theodolite via the two vector method.

Two points should be noted with regard to these procedures.

1. The calculation of the airborne component attitude was made assuming that the theodolite always remained directly above and behind the PAM measured position of the airborne component, i.e., at a fixed location. In reality, as the airborne component was reoriented, the theodolite moved slightly. The PATDS assumes that the theodolite moves with the airborne component, and that the airborne component remains in the fixed location.

2. The theodolite readings actually made are assumed to be taken with the theodolite in the same attitude. If for some reason, the attitude of the theodolite did change slightly while the readings were being made, the results calculated via the 2 vector method would not be strictly valid as one of the underlying assumptions would have been violated. Theodolite readings are assumed to be accurate; if misreadings occur, these would have the same effect of violating underlying assumptions and thereby causing erroneous calculations of the attitude.

If the results of the three pairwise computations of the principal axis and angle are averaged, and their standard deviations computed, the standard deviation gives a measure of how consistent the theodolite readings were. As can be seen for some orientations, the standard deviations are quite small and the error angles are consistently small. While for other orientations, these error angles with the accompanying larger standard deviations indicate theodolite motion or misreadings. The good performance of the best results indicates the validity of the overall technique used.

Specific Comments on the Test Results (Individual Runs)

Of the 31 runs, four appeared to have definitely moved during the time the theodolite readings were taken. Another three appeared to have theodolite misreadings on one of the points. For these runs, the most

consistent pair of readings were used to compute the attitude of the theodolite. This results in maximizing the use of the good data taken during the test.

For some as yet unknown reason, the standard deviation of the components of the principal axes unit vector appears to be much greater in one component than the others. This occurs on 9 orientations. The checks performed on the raw data indicate no obvious movement nor obvious misreadings for these 9 orientations. The very consistent small standard deviations of other runs indicates that the basic technique of using the two vector method in this manner is valid and that no problem exists in the computations performed by the various programs. This leads to the conclusion that the theodolite data may contain reading errors in the last few seconds of arc or that a very slight motion of the theodolite was made during these readings.

The analysis of the raw polarimeter data indicates a drift problem as the values were either steadily increasing or decreasing as the three runs were taken for each orientation. The relatively constant offset between the PATDS and measured mean values of C is probably due to the selection of an arbitrary zero reference, and the deliberate use of a zero offset value in the PAM computer program. The intent during the test was to compute the appropriate offset during the processing of the data to compute the correction factor. However, this was not practical due to the sudden unexplained large offset in these two angles. In view of this, it can be concluded that the polarimeter drift problem and slow response time does not meet the specifications given in the technical guidelines, however, the intent of the guidelines has been met as the feasibility of using polarization techniques in the PAM has been demonstrated. When allowed to settle in, the polarimeter has shown the capability of having the required accuracy. However, redesign to eliminate dependence on the amplitude of the received signal is necessary to achieve an operational system.

The D and E measurement subsystems are essentially identical separate subsystems, sharing only a common porro prism reflection receiver. During the test, at least two runs demonstrated the correct functioning of both subsystems (ignoring the offset problem) to within the 0.25 milliradian specifications of the technical guidelines. This validates

the overall design concept and subsystem operation. However, the majority of runs show much better operation of the D than the E subsystem. This should probably be ascribed to the dropout of the shaft angle encoder output during the test. After delivery of the system to Ft. Monmouth, this problem was diagnosed as a change in the bias level of some of the circuitry within the shaft angle encoder. This was probably due to a combination of rising temperature and vibration.

In analyzing and interpreting the data, it is apparent that test results were primarily limited by systematic errors. It is felt that many of these systematic errors were due to the angular errors induced by the engineering assumption that the various subsystems of the ground station and the airborne component were located at "the same point" rather than taking into account the distributed nature of the system. When used at the maximum intended ranges, these problems would be minimized. However, at short test ranges and for short range applications, the next version of the PAM should attempt to minimize the separations between the various subsystem and use an effectively coaxial arrangement.

The use of computerized data reduction has played a very important part in the testing and evaluation of the PAM. Without such an aid, it would have been very difficult to properly interpret the data. In addition, the PAM computer is an essential subsystem. Programming effort thus far has resulted in the development of the PAM program by Hughes and the automated data reduction system by ERADCOM. The improved attitude algorithm developed by ERADCOM will be used in future versions of the PAM. The calibration and test results which yield the necessary offsets and correction factor coefficients will be incorporated in the next version of the PAM program. Additional operational software will be added to enable the PAM computer to perform its primary mission of correcting the output of the target sensor for the attitude of the sensor and providing the necessary data for determining target location to the appropriate tactical fire control center.

The results of PAM testing have indicated good performance of the computer subsystem. Problems involving the loss of data stored on disc during the test were traced to a subtle interrupt timing problem and have since been corrected.

The analysis of the pre-acceptance test data in detail has resulted in the ability to answer several major questions regarding the PAM equipment and the test techniques used.

Conclusions

Based on the performance of the PAM through pre-acceptance testing, it can be stated that the basic feasibility of the PAM has been successfully demonstrated. The pointing and tracking, range measurement, pitch/yaw, polarization measurement, and computer subsystem have each individually demonstrated their capacity to perform their respective functions within the levels demanded by the technical guidelines. However, the use of modified commercial hardware bolted together as the exploratory development model of the PAM has resulted in problems which are characteristic of the particular hardware used rather than the PAM design.

Test data analysis has shown that if each subsystem were to perform at its best, a system would result which would have met the technical guidelines in attitude accuracy of 0.25 milliradians. This would be an improvement in the state of the art from inertial attitude reference systems capable of 0.5 degree accuracy (8.5 milliradians) by a factor of almost 40. Even with the problems encountered, the overall accuracy of the PAM is on the order of 1 milliradian, for almost an order of magnitude improvement in the current state of the art.

Novel test, alignment, and analysis techniques have been developed during this effort which represent a significant improvement in the state of the art in their own right over previous methods. Based on the above, the exploratory development of the PAM can be considered as a success and further development is warranted in order to achieve a fieldable PAM.

STATIC TEST ORIENTATION # 1

	C	D	E
MEAN	.478911	1.390770	1.397260
+ OR -	.000200	.000120	.000080
PATDS	.004858	-.104006	.104068
DIFFERENCE	.474053	1.494780	1.293190

PAR:	.703862	-.707268	.065958	AR:	.155393
STD:	.000480	.002500	.026000		.000300

THEODOLITE		PATDS		ANGULAR
AZ	EL	AZ	EL	ERROR
-104.72	104.72	-104.62	104.69	.10
-70.27	111.50	-70.33	111.15	.36
-140.60	110.59	-140.34	110.02	.63

STATIC TEST ORIENTATION # 2

	C	D	E
MEAN	.477590	1.496570	1.393850
+ OR -	.000310	.000110	.004300
PATDS	.000000	.001324	.104671
DIFFERENCE	.477590	1.495250	1.289180

PAR:	.035579	-.999366	.001711	AR:	.110844
STD:	.000320	.000560	.006000		.000070

THEODOLITE		PATDS		ANGULAR
AZ	EL	AZ	EL	ERROR
-104.72	.00	-104.61	.00	.11
-70.41	6.30	-70.43	6.34	.04
-140.32	6.19	-140.04	6.15	.28

STATIC TEST ORIENTATION # 3

	C	D	E
MEAN	.473680	1.889230	1.412860
+ OR -	.000440	.760000	.016000
PATDS	-.005371	.106590	.104795
DIFFERENCE	.479051	1.782640	1.308060

PAR: -.676556 -.732372 -.076829 AR: 1.500340
STD: .000280 .004300 .039000 .000490

THEODOLITE		PATDS		ANGULAR
AZ	EL	AZ	EL	ERROR
104.72	104.72	104.73	104.63	.09
70.19	98.54	70.28	98.80	.28
140.46	97.89	140.22	97.89	.24

STATIC TEST ORIENTATION # 4

	C	D	E
MEAN	.478550	1.566330	1.433670
+ OR -	.000340	.000085	.009900
PATDS	.004422	.071327	.069949
DIFFERENCE	.474128	1.495000	1.363720

PAR: -.656683 -.750595 -.073314 AR: .100800
STD: .000930 .006100 .064000 .000550

THEODOLITE		PATDS		ANGULAR
AZ	EL	AZ	EL	ERROR
69.81	69.81	69.91	69.79	.10
35.42	63.39	35.60	63.74	.39
105.51	63.24	105.35	63.24	.16

STATIC TEST ORIENTATION # 5

	C	D	E
MEAN	.477747	1.037120	1.431390
+ OR -	.000210	.000210	.000150
PATDS	.075960	.106318	.069913
DIFFERENCE	.401787	.930802	1.361480

PAR: -.799676 -.593129 -.093362 AR: .126635
STD: .002200 .005900 .052000 .000699

THEODOLITE		PATDS		ANGULAR
AZ	EL	AZ	EL	ERROR
-69.81	-104.72	-69.87	-104.69	.07
-35.31	-98.43	-35.43	-98.60	.39
-105.58	-98.06	-105.38	-97.91	.25

STATIC TEST ORIENTATION # 6

	C	D	E
MEAN	.483621	1.461420	1.466710
+ OR -	.000200	.000000	.018000
PATDS	.004340	-.033658	.034910
DIFFERENCE	.479281	1.495080	1.431800

PAR: .686952 -.721725 8.490721 AR: .056711
STD: .002600 .004100 .051000 .000280

THEODOLITE		PATDS		ANGULAR
AZ	EL	AZ	EL	ERROR
-34.91	34.91	-34.89	34.94	.04
-.62	41.38	-.72	41.42	.11
-70.56	41.14	-70.38	40.89	.31

STATIC TEST ORIENTATION # 7

	C	D	E
MEAN	.483944	1.496210	1.465510
+ OR -	.000280	.000000	.000610
PATDS	.000691	.001285	.034941
DIFFERENCE	.483253	1.494930	1.430570

PAR:	.096149	-.995339	.007494	AR:	.041236
STD:	.001400	.001100	.056000		.000086

THEODOLITE		PATDS		ANGULAR
AZ	EL	AZ	EL	ERROR
-34.91	.00	-34.92	.03	.03
-.65	6.43	-.75	6.37	.12
-70.51	6.27	-70.35	6.18	.18

STATIC TEST ORIENTATION # 8

	C	D	E
MEAN	.483640	1.531360	1.465920
+ OR -	.000480	.000000	.002300
PATDS	.000000	.036214	.034892
DIFFERENCE	.483640	1.495150	1.431030

PAR:	-.602973	-.797484	-.021042	AR:	.051360
STD:	.000280	.001400	.036000		.000120

THEODOLITE		PATDS		ANGULAR
AZ	EL	AZ	EL	ERROR
-34.91	-34.91	-34.87	-31.36	3.55
.59	-28.43	.67	-28.56	.15
70.54	-28.74	70.31	-28.61	.26

STATIC TEST ORIENTATION # 9

	C	D	E
MEAN	.486246	1.513450	1.482190
+ OR -	.000210	.000100	.002500
PATDS	.239200	.189230	.017841
DIFFERENCE	.247046	1.324220	1.464350

PAR:	-.494711	-.863858	-.094922	AR:	.027677
STD:	.008200	.021000	.180000		.000690

THEODOLITE		PATDS		ANGULAR
AZ	EL	AZ	EL	ERROR
-17.45	-17.45	-17.83	-17.59	.40
16.86	-10.91	16.83	-11.35	.44
-53.07	-11.08	-53.25	-11.32	.30

STATIC TEST ORIENTATION # 10

	C	D	E
MEAN	.486817	1.496230	1.489490
+ OR -	.000100	.000100	.027000
PATDS	.001953	.001212	.017745
DIFFERENCE	.484864	1.495020	1.471750

PAR:	.166578	-.982599	.082168	AR:	.024000
STD:	.005200	.017000	.160000		.000480

THEODOLITE		PATDS		ANGULAR
AZ	EL	AZ	EL	ERROR
-17.45	.00	-17.74	.11	.31
16.86	6.54	16.63	6.50	.23
-53.05	6.30	-53.18	6.20	.16

STATIC TEST ORIENTATION # 11

	C	D	E
MEAN	.487335	1.478430	1.484440
+ OR -	.000068	.020000	.000089
PATDS	.001092	-.017042	.183040
DIFFERENCE	.486243	1.495470	1.301400

PAR:	.674282	-.738130	.022562	AR:	.033055
STD:	.021000	.019500	.267300		.000960

THEODOLITE		PATDS		ANGULAR
AZ	EL	AZ	EL	ERROR
-17.45	17.45	-18.29	18.35	1.23
16.91	23.95	15.88	24.69	1.27
-53.01	24.10	-53.74	24.47	.82

STATIC TEST ORIENTATION # 12

	C	D	E
MEAN	.487125	1.036800	1.500940
+ OR -	.000340	.000200	.000060
PATDS	-.007421	.114719	.000719
DIFFERENCE	.494546	.922081	1.500220

PAR:	-.995766	-.057858	-.071437	AR:	.109919
STD:	.060000	.021000	.392921		.006230

THEODOLITE		PATDS		ANGULAR
AZ	EL	AZ	EL	ERROR
.00	-104.71	-.72	-113.34	8.66
34.42	-98.24	33.70	-107.20	8.99
-35.79	-98.36	-36.31	-106.82	8.48

STATIC TEST ORIENTATION # 13

	C	D	E
MEAN	.489418	1.531410	1.501140
+ OR -	.000200	.000200	.000200
PATDS	-.005546	.036228	.000004
DIFFERENCE	.494964	1.495180	1.501140

PAR:	-.966412	-.186926	-.176372	AR:	.032043
STD:	.361275	.078000	.332674		.088620

THEODOLITE		PATDS		ANGULAR
AZ	EL	AZ	EL	ERROR
.00	-34.91	.00	-34.88	.03
34.29	-28.39	34.28	-28.73	.34
-35.64	-28.58	-35.42	-28.50	.23

STATIC TEST ORIENTATION # 14

	C	D	E
MEAN	.490203	1.513650	1.517420
+ OR -	.000200	.000180	.023000
PATDS	-.010507	.020180	.000705
DIFFERENCE	.500710	1.493470	1.516720

PAR:	.895085	.401617	.193716	AR:	.015104
STD:	.161381	.075000	.260493		.012900

THEODOLITE		PATDS		ANGULAR
AZ	EL	AZ	EL	ERROR
.00	-17.45	-.70	-18.85	1.57
34.29	-10.98	33.53	-12.87	2.04
-35.61	-11.17	-36.08	-12.29	1.21

STATIC TEST ORIENTATION # 15

	C	D	E
MEAN	.491040	1.496020	1.501380
+ OR -	.000280	.000400	.000620
PATDS	.003312	.000788	.000726
DIFFERENCE	.487728	1.495230	1.500650

PAR:	.503748	-.774521	.382563	AR:	.008828
STD:	.084000	.124199	.359260		.001700

THEODOLITE AZ	THEODOLITE EL	PATDS AZ	PATDS EL	ANGULAR ERROR
.00	.00	-.73	.53	.90
34.22	6.55	33.43	6.97	.89
-35.70	6.37	-36.18	6.58	.52

STATIC TEST ORIENTATION # 16

	C	D	E
MEAN	.491250	1.478620	1.507680
+ OR -	.000079	.000620	.008900
PATDS	.032453	-.031014	.004308
DIFFERENCE	.458797	1.509630	1.503370

PAR:	.728347	-.200817	.655120	AR:	.049737
STD:	.313671	.090000	.340701		.035054

THEODOLITE AZ	THEODOLITE EL	PATDS AZ	PATDS EL	ANGULAR ERROR
.00	17.45	-4.31	32.31	15.47
34.39	24.02	29.67	39.72	16.39
-35.57	23.87	-39.94	37.30	14.12

STATIC TEST ORIENTATION # 17

	C	D	E
MEAN	.491284	1.461120	1.501740
+ OR -	.000110	.000080	.000180
PATDS	.000000	-.054142	.003156
DIFFERENCE	.491284	1.515260	1.498580

PAR: .988046 -.154108 -.004091 AR: .060105
STD: .218992 .025000 .640935 .023000

THEODOLITE		PATDS		ANGULAR
AZ	EL	AZ	EL	ERROR
.00	34.91	-3.15	55.42	20.75
34.28	41.30	31.08	61.70	20.65
-35.66	41.18	-38.65	61.56	20.60

STATIC TEST ORIENTATION # 18

	C	D	E
MEAN	.490618	1.391000	1.501720
+ OR -	.000200	.000100	.000400
PATDS	-.016173	-.103399	.000018
DIFFERENCE	.506791	1.494400	1.501700

PAR: .987580 -.062769 -.144008 AR: .110056
STD: .361282 .002400 .390721 .196108

THEODOLITE		PATDS		ANGULAR
AZ	EL	AZ	EL	ERROR
.00	104.72	-.02	104.65	.07
34.44	111.29	34.02	110.34	1.04
-35.89	111.16	-35.56	111.31	.36

STATIC TEST ORIENTATION # 19

	C	D	E
MEAN	.492561	1.478500	1.632750
+ OR -	.000120	.000190	.100000
PATDS	.000000	-.016134	-.017456
DIFFERENCE	.492561	1.494630	1.650210

PAR:	.883193	.468940	-.008071	AR:	.024207
STD:	.415220	.214852	.816174		.623744

THEODOLITE		PATDS		ANGULAR
AZ	EL	AZ	EL	ERROR
17.45	17.45	17.45	17.44	.01
51.72	23.91	51.63	23.74	.19
18.19	23.78	17.99	23.61	.27

STATIC TEST ORIENTATION # 20

	C	D	E
MEAN	.493030	1.496320	1.398160
+ OR -	.000200	.000100	.339141
PATDS	-.001691	.001129	-.017872
DIFFERENCE	.494721	1.495190	1.416030

PAR:	.328210	.934440	-.138204	AR:	1.260190
STD:	.014000	.038500	.246214		.000541

THEODOLITE		PATDS		ANGULAR
AZ	EL	AZ	EL	ERROR
17.45	.00	17.86	.19	.45
51.70	6.42	52.04	6.45	.34
-18.22	6.27	-17.56	6.42	.68

STATIC TEST ORIENTATION # 21

	C	D	E
MEAN	.493648	1.513780	1.623870
+ OR -	.000006	.000070	.114000
PATDS	.005051	.018988	-.017676
DIFFERENCE	.488597	1.494790	1.641550

PAR:	-.737649	.615146	.278332	AR:	.018714
STD:	.034000	.033000	.153095		.000970

THEODOLITE		PATDS		ANGULAR
AZ	EL	AZ	EL	ERROR
17.45	-17.45	17.69	-17.65	.31
51.69	-10.94	51.81	-11.13	.22
-18.18	-11.11	-17.80	-11.66	.67

STATIC TEST ORIENTATION # 22

	C	D	E
MEAN	.494690	1.531020	1.394960
+ OR -	.000340	.000620	.214000
PATDS	.004956	.036378	-.035089
DIFFERENCE	.489734	1.494640	1.430050

PAR:	-.728245	.672774	.130511	AR:	.042890
STD:	.007800	.011000	.091000		.000580

THEODOLITE		PATDS		ANGULAR
AZ	EL	AZ	EL	ERROR
34.91	-34.91	35.07	-35.01	.19
69.17	-28.33	69.21	-28.45	.13
-.77	-28.54	-.42	-29.04	.61

AD-A079 540 HUGHES AIRCRAFT CO CULVER CITY CALIF F/G 17/8
POSITION AND ATTITUDE MONITOR (PAM).(U)
AUG 79 L HILL, W BUCHMAN, J WAGNER, R JULIAN DAAB07-75-C-0810
UNCLASSIFIED HAC-FR-79-73-801R DELNV-TR-75-0810-F NL

2 OF 2
AD A079540

END
DATE FILMED
3-80
DDC

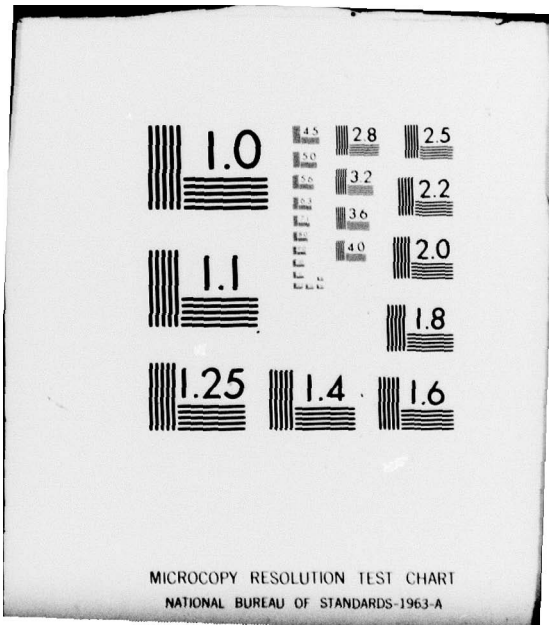
1.0
1.1
1.25
1.4
1.6
2.0
2.2
2.5
2.8
3.2
3.6
4.0
4.5
5.0
5.6
6.3
MICROCOPY RESOLUTION TEST CHART
NATIONAL BUREAU OF STANDARDS-1963-A

STATIC TEST ORIENTATION # 23

	C	D	E
MEAN	.495344	1.496080	1.562770
+ OR -	.000200	.000620	.026100
PATDS	-.000488	.001173	-.035420
DIFFERENCE	.495832	1.494910	1.598190

PAR:	.137752	.990428	-.008774	AR:	.029602
STD:	.006200	.011000	.180985		.000310

THEODOLITE		PATDS		ANGULAR
AZ	EL	AZ	EL	ERROR
34.91	.00	35.39	.15	.50
69.14	6.55	69.57	6.46	.44
-.76	6.38	-.04	6.32	.72

STATIC TEST ORIENTATION # 24

	C	D	E
MEAN	.495241	1.461130	1.495440
+ OR -	.000170	.000090	.028000
PATDS	-.006659	-.034368	-.035380
DIFFERENCE	.501900	1.495500	1.530820

PAR:	.798031	.585424	-.142916	AR:	.049807
STD:	.022000	.020000	.169008		.001540

THEODOLITE		PATDS		ANGULAR
AZ	EL	AZ	EL	ERROR
34.91	34.91	35.36	35.64	.86
69.19	41.40	69.60	41.67	.49
-.75	41.31	-.06	42.06	1.02

STATIC TEST ORIENTATION # 25

	C	D	E
MEAN	.494416	1.436870	1.575870
+ OR -	.000200	.015000	.009000
PATDS	-.005900	-.068420	-.069969
DIFFERENCE	.500316	1.505290	1.645840

PAR:	.758096	.647113	-.080845	AR:	.098121
STD:	.003000	.006500	.068000		.000640

THEODOLITE		PATDS		ANGULAR
AZ	EL	AZ	EL	ERROR
69.81	69.81	69.93	70.05	.27
104.17	76.07	104.25	75.95	.14
34.08	76.25	34.46	76.54	.48

STATIC TEST ORIENTATION # 26

	C	D	E
MEAN	.499660	1.566290	1.288910
+ OR -	.000240	.000200	.087000
PATDS	.005051	.071341	-.069896
DIFFERENCE	.494609	1.494950	1.358810

PAR:	-.720225	.688934	.081523	AR:	.092009
STD:	.000690	.002700	.027000		.000210

THEODOLITE		PATDS		ANGULAR
AZ	EL	AZ	EL	ERROR
69.81	-69.81	69.85	-69.81	.04
104.11	-63.14	104.03	-63.14	.08
34.06	-63.64	34.28	-63.94	.37

STATIC TEST ORIENTATION # 27

	C	D	E
MEAN	.504220	1.348080	1.578360
+ OR -	.000560	.420000	.029000
PATDS	.007437	.106689	.104888
DIFFERENCE	.496783	1.241390	1.473470

PAR:	-.718505	.689478	.091491	AR:	.141649
STD:	.000400	.004800	.036000		.000530

THEODOLITE		PATDS		ANGULAR
AZ	EL	AZ	EL	ERROR
104.72	-104.72	104.82	-104.73	.10
139.12	-97.79	139.04	-97.70	.12
68.88	-98.76	69.97	-99.15	1.15

STATIC TEST ORIENTATION # 28

	C	D	E
MEAN	.503018	1.496050	1.606060
+ OR -	.000600	.000260	.000210
PATDS	.000691	.001264	-104.841995
DIFFERENCE	.502327	1.494790	106.447997

PAR:	.040179	.999182	.004471	AR:	.098820
STD:	.002500	.000790	.042000		.000049

THEODOLITE		PATDS		ANGULAR
AZ	EL	AZ	EL	ERROR
104.72	.00	104.78	.06	.08
138.97	6.50	138.97	6.39	.11
69.07	6.33	69.34	6.32	.27

STATIC TEST ORIENTATION # 29

	C	D	E
MEAN	.499509	1.390790	1.605780
+ OR -	.000400	.000100	.000580
PATDS	-.004448	-.104237	-.104856
DIFFERENCE	.503957	1.495030	1.710640

PAR:	.744425	.664685	-.063443	AR:	.147282
STD:	.001000	.005200	.052000		.000580

THEODOLITE		PATDS		ANGULAR
AZ	EL	AZ	EL	ERROR
104.72	104.72	104.79	104.91	.20
139.22	110.85	139.25	110.64	.21
68.91	111.37	69.23	111.55	.37

STATIC TEST ORIENTATION # 30

	C	D	E
MEAN	.510189	1.499620	1.607130
+ OR -	.002200	.000170	.000350
PATDS	-.000488	.004655	-.106172
DIFFERENCE	.510677	1.494970	1.713300

PAR:	.006236	.999980	-.001330	AR:	.100073
STD:	.002300	.000000	.039000		.000000

THEODOLITE		PATDS		ANGULAR
AZ	EL	AZ	EL	ERROR
106.05	-3.36	106.11	-3.31	.08
140.32	3.06	140.27	3.01	.07
70.41	2.98	70.67	2.86	.29

STATIC TEST ORIENTATION # 31

	C	D	E
MEAN	.521102	1.501020	1.497440
+ OR -	.001400	.000260	.003600
PATDS	-.001196	.006485	.002853
DIFFERENCE	.522298	1.494530	1.494590

PAR:	-.135764	.684780	.091491	AR:	.141649
STD:	.007500	.067000	.360000		.000720

THEODOLITE		PATDS		ANGULAR
AZ	EL	AZ	EL	ERROR
-2.22	-5.13	-2.85	5.16	10.31
32.05	1.31	31.33	1.12	.74
-37.86	1.21	-38.27	1.05	.44

8.0 GLOSSARY AND PAM DESIGN SPECIFICATIONS

AC	PAM Airborne Component
GA	Gimbal Assembly
GS	PAM Ground Station
LOS	Line of sight between ground station and airborne component
PALS-A	Airborne Passive Artillery Locating System
RPV	Remotely Piloted Vehicle
Pitch	angle measured by spinning porro prism shaft angle encoder giving direction to ground station (Note difference from standard definition) in airborne component XZ plane
Yaw	angle measured by spinning porro prism shaft angle encoder giving direction to ground station (Note difference from standard definition) in airborne component YZ plane
Roll	apparent angle of rotation of the polaroid filter pass axis about the line of sight (Note difference from standard definition)

PAM DESIGN SPECIFICATIONS

Airborne Component

Maximum total weight	≤15 pounds
Mounting Surface Size	= 2 ft by 2 ft
Available Power	115 volts, 1 phase, 60 Hz 115 volts, 3 phase, 400 Hz 28 volts DC

Ground Equipment

Rack-mounted equipment.

Support structure should not introduce measuring errors.

Sensor adapted to look in horizontal direction for tests.

Operation against sky background shall not degrade performance.

System Requirements and Performance

Provide search mode to establish lock-on and track airborne system.

Operationable day or night with visibility 3 km or better.

Extension to covert wavelength must be possible.

Angular accuracy ≤ 0.25 mrad (1σ).

Position accuracy Δy_o, Δx_o ± 1 meter.

Δz_o $\leq \pm 0.5$ meter.

Provide hard copy of output data when system is "flashed."

Sufficiently rugged to survive normal field tests.